



# The impact of tumor microenvironment: unraveling the role of physical cues in breast cancer progression

Ayuba Akinpelu<sup>1</sup> · Tosin Akinsipe<sup>2</sup> · L. Adriana Avila<sup>2</sup> · Robert D. Arnold<sup>3</sup> · Panagiotis Mistriotis<sup>1</sup>

Received: 22 August 2023 / Accepted: 2 January 2024 / Published online: 19 January 2024  
© The Author(s) 2024

## Abstract

Metastasis accounts for the vast majority of breast cancer-related fatalities. Although the contribution of genetic and epigenetic modifications to breast cancer progression has been widely acknowledged, emerging evidence underscores the pivotal role of physical stimuli in driving breast cancer metastasis. In this review, we summarize the changes in the mechanics of the breast cancer microenvironment and describe the various forces that impact migrating and circulating tumor cells throughout the metastatic process. We also discuss the mechanosensing and mechanotransducing molecules responsible for promoting the malignant phenotype in breast cancer cells. Gaining a comprehensive understanding of the mechanobiology of breast cancer carries substantial potential to propel progress in prognosis, diagnosis, and patient treatment.

**Keywords** Breast cancer mechanobiology · Physical signals · Tumor microenvironment · Metastasis

## 1 Introduction

According to the Centers for Disease Control and Prevention, breast cancer is the second leading cause of death among women in the US. Breast cancers are often classified based on their invasive potential. Ductal carcinoma *in situ* is a non-invasive type of breast cancer characterized by the uncontrolled proliferation of neoplastic epithelial cells, which remain localized within the mammary ducts [1]. In contrast, invasive breast cancers originate primarily in the milk ducts (invasive ductal carcinoma) or breast lobules (invasive lobular carcinoma) and can spread to nearby breast tissues or even metastasize to other body parts [1, 2]. Breast cancers can also be categorized into different subtypes based on the expression levels of the human epidermal growth factor receptor 2 (HER2) and two hormone

receptors: estrogen receptor (ER) and progesterone receptor (PR). Luminal-like tumors (luminal A and luminal B) make up ~70% of all breast tumors [3–5]. Luminal A tumors are generally associated with a more favorable prognosis and typically express ER and PR. In contrast, luminal B tumors, while also expressing ER, display lower expression of PR and exhibit a higher rate of proliferation than luminal A tumors, resulting in a less favorable prognosis [3–5]. HER2 positive tumors, which comprise ~15% of all breast cancers, express high levels of HER2 but lack ER, and PR expression [3–5]. These tumors are associated with a less favorable outlook compared to luminal tumors. Triple-negative breast cancer (~15% of all breast cancers) lacks expression of ER, PR, and HER2, making targeted therapies ineffective and resulting in worse survival rates compared to other subtypes [3–5].

The lack of strategies to clinically interrupt and treat the metastatic spread of tumor cells accounts for the vast majority of breast cancer-associated deaths. This is supported by data showing that the 5-year survival rate for women diagnosed with distant-stage breast cancer is 29% versus 85–99% for those diagnosed with local- or regional-stage disease [6]. During metastasis, a tiny fraction of tumor cells splits away from the primary tumor region enters the circulation (intravasation) and exits (extravasation) to form a secondary tumor at a distant region (Fig. 1) [7, 8]. These migrating or circulating tumor cells are exposed to various

✉ Panagiotis Mistriotis  
pmistriotis@auburn.edu

<sup>1</sup> Department of Chemical Engineering, Samuel Ginn College of Engineering, Auburn University, Auburn, AL 36849, USA

<sup>2</sup> Department of Biological Sciences, College of Science and Mathematics, Auburn University, Auburn, AL 36849, USA

<sup>3</sup> Department of Drug Discovery and Development, Harrison College of Pharmacy, Auburn University, Auburn, AL 36849, USA

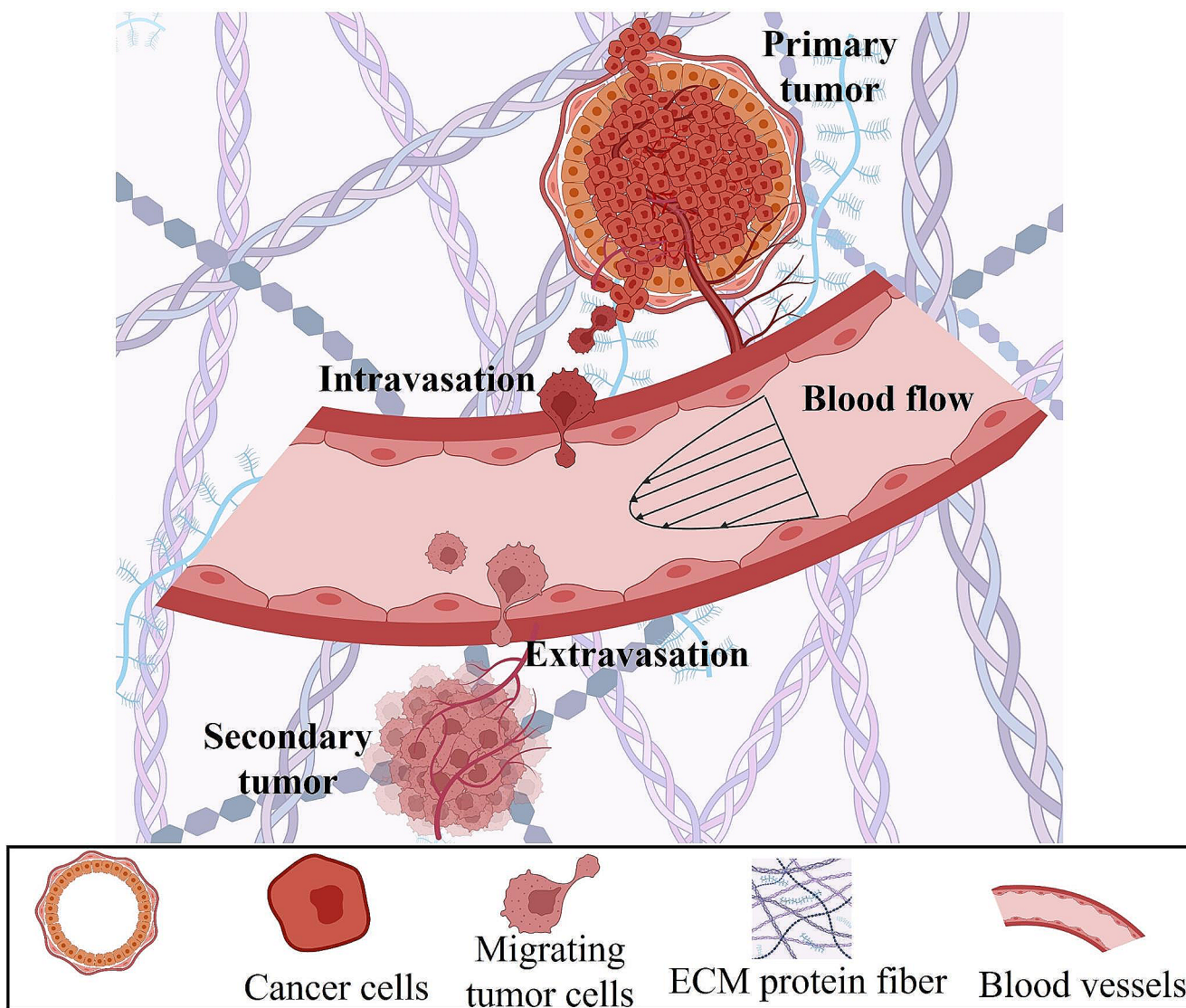


**Fig. 1** Schematic illustrating the multi-step process of breast cancer metastasis, with tumor cells escaping the primary tumor, entering the circulation, and extravasating to form a secondary tumor

physical cues, including interstitial fluid pressure, matrix stiffness, solid stress, viscoelasticity, confining 3D topographies, hydraulic resistance, extracellular fluid viscosity, and drag forces (Fig. 2; Table 1) [9, 10].

Emerging evidence demonstrates that tumor cells possess the ability to sense and interpret these signals through mechanosensors and mechanotransducers, including mechanosensitive ion channels (e.g., ion channels that belong to the transient receptor potential (TRP) family), ion transporters, focal adhesions, cytoskeletal elements, nuclear proteins, and transcription factors. In response to physical stimuli, these molecules can initiate signal transduction, modulate the intracellular ion concentration (e.g., calcium, sodium, and chloride), influence cellular tension, volume, and shape, and trigger transcriptional changes, thereby contributing to

therapeutic resistance and mediating profound changes in cellular functions, including division, and migration (see sections below). This review describes the contributions of the aforementioned physical cues to breast tumor progression and discusses the underlying mechanosensing mechanisms. In our opinion, unraveling the diverse mechanoresponses of breast tumor cells will facilitate the development of new therapeutic approaches to combat breast cancer progression.

## Migrating and Circulating Tumor Cells Encounter Diverse Physical Cues

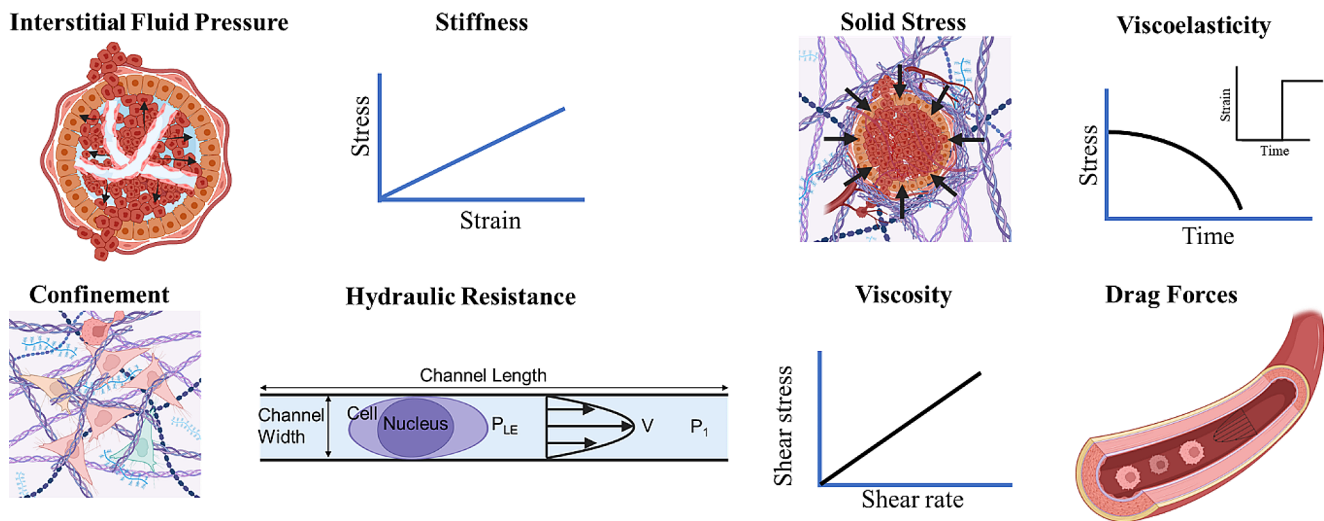


**Fig. 2** Throughout the metastatic cascade, breast tumor cells encounter a diverse array of physical cues that profoundly influence their behavior. These include interstitial fluid pressure, matrix stiffness, solid

stress, viscoelasticity, confining 3D topographies, hydraulic resistance, extracellular fluid viscosity, and drag forces.  $P_{LE}$ : hydraulic pressure at the cell leading-edge;  $V$ : fluid velocity;  $P_1$ : upstream pressure

**Table 1** Description of different physical cues experienced by breast cancer cells during tumor progression and metastasis

Physical stimuli	Definition
Interstitial fluid pressure (IFP)	The pressure exerted by the interstitial fluid on cancer cells
Extracellular matrix (ECM) stiffness	The resistance of the extracellular matrix to deformation when stress is applied
Solid stress	Compressive Stress: The force per area exerted by the surrounding tissue on tumors as they grow Residual Stress: The force per area generated due to intratumoral cell-cell and cell-ECM interactions
Viscoelasticity	A characteristic feature of living tissues that exhibit both viscous and elastic behavior
Cellular Confinement	Spatial restrictions imposed on cells during migration and metastasis
Hydraulic resistance	The external load that resists fluid movement
Viscosity	A measure of the fluid's resistance to deformation under the influence of shear stress
Drag forces	Tangential (shear) or normal (pressure) forces exerted by the moving fluid on cells

**Table 2** IFP measurements in normal and abnormal breast tissues using the wick-in-needle technique

Breast Tissue	IFP (mmHg)		hormone-independent LM3 murine breast cancer cells	$2.9 \pm 0.4$ [54]
	Human	Mouse		
Normal Breast Parenchyma	$-0.3 \pm 0.1$ [12]		$\sim 0$ [20]	
Benign conditions	$0.4 \pm 0.4$ [12]			
	$3.6 \pm 0.8$ [12]			
Breast Carcinoma	Non-invasive	$-0.3 \pm 0.2$ [12]	hormone-dependent MCF-7 human breast cancer cells	$14 \pm 10$ [24]
	Tumor stage (T2-T4)	$15 \pm 9$ [19]	triple-negative MDA-MB-231 breast cancer cells	$19.4 \pm 3$ [20]
	Invasive	$29 \pm 3$ [12]	triple-negative MDA-MB-231 breast cancer cells	$\sim 11$ [55]
			triple negative MDA-MB-468 breast cancer cells	$\sim 8$ [55]

## 2 Interstitial fluid pressure

The hydrostatic and osmotic pressure differences between the vasculature and the surrounding tissue move fluid out from the blood vessels to the interstitium, allowing the supply of nutrients and oxygen to the resident tissue cells [11]. The lymphatic system serves the purpose of maintaining

interstitial fluid homeostasis and removing unwanted waste products. As a result, the IFP of normal breast parenchyma is  $\sim 0$  mm Hg [12]. The increased demands of growing tumors in nutrients and oxygen triggers the formation of new blood vessels, a process called angiogenesis. The tumors' tortuous and hyperpermeable vessels [13–16] and the near absence of functional lymphatic vessels [17, 18] raise the interstitial fluid pressure (IFP) within breast tumors (Table 2). Using

a small number of patients, Jain's group has reported that IFP scales with breast tumor aggressiveness [19]. In this study, the IFP range was between 4 and 33 mm Hg, with the highest pressure measurements recorded in advanced breast tumors [19]. These findings have been corroborated by others, who have demonstrated elevated IFP in invasive ductal carcinomas relative to benign tumors or noninvasive carcinomas and a positive correlation between tumor size and IFP [12]. In addition to human breast tumors, IFP increases in experimental models of breast cancer, such as severe combined immunodeficient mice bearing highly invasive, triple-negative MDA-MB-231 human breast cancer tumors [20] and BN472 rat mammary carcinomas [21].

Micropuncture and wick-in-needle are the gold standard techniques for measuring IFP. Despite yielding the most reliable values and being less traumatic, micropuncture is limited by its depth of penetration which does not exceed 1 mm [11]. Thus, researchers gravitate towards the wick-in-needle technique which enables deeper penetration. Noninvasive methods for assessing IFP include intravoxel incoherent motion-diffusion weighted imaging [22], ultrasound poroelastography [23] and contrast-enhanced magnetic resonance imaging [24].

Although the IFP is relatively uniform throughout the breast tumor, it decreases significantly at its edge [25]. This pressure gradient triggers outward convection, creating a barrier to effective drug delivery [26, 27] and influencing breast cancer cell behavior (see also the "Drag forces" section below). A strategic way to circumvent the impaired transport of therapeutic agents is to reduce IFP and thereby improve tumor perfusion. This can be achieved using antiangiogenic agents which promote vascular normalization [28, 29]. For instance, the administration of the anti-VEGF-receptor-2 antibody DC101 enhances penetration of therapeutic molecules and nanomedicines up to the size of ~12 nm [30]. Abraxane, formulated with albumin-bound nanoparticles and the cancer chemotherapy agent paclitaxel, is a nanomedicine within this size range that has been effective in breast cancer treatments [30–32]. Targeting VEGF due to its over-secretion during tumor progression has also prompted the use of bevacizumab, an anti-human VEGF monoclonal antibody that reduces the growth of tumor vessels [33, 34]. Bevacizumab has been used in many breast cancer clinical trials in combination with chemotherapy. However, these combination therapies have not shown a significant increase in overall survival compared to chemotherapy alone [35–38]. This lack of significant improvement may be attributed to the activation of VEGF-independent angiogenic pathways, the recruitment of proangiogenic stromal cells, the induction of vasculogenesis or even the dose of the antiangiogenic agent used, which may reduce the size of blood vessel pores, further obstructing the delivery of this

antibody [30, 39, 40]. In addition to antiangiogenic agents, certain chemotherapeutic agents have shown promising results in suppressing IFP. Taxanes, such as paclitaxel and docetaxel have been found to inhibit angiogenesis at low concentrations [41–44], and promote vascular decompression, effectively suppressing IFP in mouse mammary carcinoma [45]. These positive outcomes have been extended to breast cancer patients, where paclitaxel administration resulted in a ~40% reduction in IFP and improved tumor oxygenation [46]. However, it is important to note that not all chemotherapeutic agents have the same impact. For instance, doxorubicin does not elicit significant effects on oxygen levels and fails to ameliorate IFP in breast cancer patients [46].

Despite the well-established increase in IFP within breast tumors, our understanding of how breast cancer cells respond to this physical stimulus remains elusive due to the scarcity of reliable in vitro platforms that permit adjustment of pressure independent of changes in pH or the dissolved concentration of gases. Moreover, experiments are often performed under supraphysiological pressures [47–49] that are orders of magnitude larger than those sensed by tumor cells *in vivo*. Recent work has revealed that breast tumor cells possess the ability to detect subtle hydrostatic pressure changes, as low as 0.02 mmHg [50]. This extraordinary sensitivity is mediated by the activation of the mechanosensitive transient receptor potential cation channel subfamily M member 7 (TRPM7), which in turn triggers calcium ions ( $\text{Ca}^{2+}$ ) influx, thereby promoting a thicker actomyosin cortex [50]. Considering these intriguing findings, it is reasonable to expect that the substantially higher IFP levels found within tumors would have a profound impact on tumor cell behavior. Indeed, exposure of tumor cells to elevated, yet physiologically relevant, pressure, using a pressurized cultured system that maintains a constant pH, has been found to increase or decrease cell proliferation, depending on the cancer cell type [51]. Moreover, increased pressure has been shown to enhance cancer cell migration and resistance to the anticancer drug doxorubicin by upregulating the water channel aquaporin 1 [52] and the efflux transporter ABCC1 [53], respectively. Further research is needed to fully elucidate the effects of IFP on breast cancer metastasis as well as the mechanisms governing pressure-induced responses.

### 3 Extracellular matrix stiffness

The extracellular matrix (ECM) is a key component of the tumor microenvironment, providing structural support and acting as a reservoir of cues, including biophysical signals such as matrix stiffness and viscoelasticity. The ECM of the healthy mammary gland includes glycosaminoglycans and

proteoglycans (e.g., hyaluronan and versican), fibrillar collagens (e.g., type I and type III collagen), basement membrane proteins (e.g., collagen type IV and laminins), and fibronectin [56]. During breast cancer, tumor cells recruit resident fibroblasts [57], adipocytes [58], and/or bone marrow-derived mesenchymal stem cells [59], transforming them into cancer-associated fibroblasts (CAFs), which in turn reshape and remodel the tumor microenvironment. To induce this transformation, tumor cells secrete signaling molecules (e.g., Wnt7a [60], and osteopontin [61, 62]), and release exosomes containing miRNAs (e.g., miR-9 [63] or miR-125b [64]) and proteins like survivin [65].

Typically, CAFs overexpress alpha-smooth muscle actin ( $\alpha$ -SMA), Vimentin, platelet-derived growth factor receptor  $\alpha$  (PDGFR $\alpha$ ), PDGFR $\beta$ , Tenascin-C, Caveolin 1, fibroblast activation protein (FAP), and ferroptosis suppressor protein 1 (FSP1) [66]. However, it is important to note that while these markers are commonly associated with CAFs, they are not limited exclusively to this cell type. Other cell types, such as normal fibroblasts, smooth muscle cells, and pericytes, also express them. In addition to their role in promoting breast cancer cell proliferation [67] and mediating inflammation [68], breast CAFs deposit collagen type I and fibronectin [58], secrete matrix metalloproteinases (MMPs) [69], and promote collagen crosslinking (e.g., via lysyl oxidase (LOX)) [70]. These alterations in the tumor ECM induce an increase in its stiffness, typically evaluated using techniques that either require direct contact with the sample (e.g., atomic force microscopy), or measure the tumor mechanical properties in a contact-free manner (e.g., shear wave elastography, magnetic resonance elastography)

(Table 3). Besides CAFs, breast cancer cells can also trigger ECM stiffening by increasing the tension of ECM fibers [71]. The quantification of ECM stiffness can serve as a valuable diagnostic and prognostic marker for breast cancer [72–74], improving physicians' clinical assessment of tumor status and their capability to predict patient outcomes.

Stiffness measurements have demonstrated that the invasive front of HER2 positive and triple-negative human breast cancers is stiffer compared to luminal A and luminal B breast tumors [75]. Elevated stiffness promotes breast tumor progression by increasing angiogenesis and vascular permeability [76] as well as breast cancer cell proliferation [77], stemness [78], and metastasis [70]. Importantly, matrix stiffness can activate the epithelial to mesenchymal transition (EMT) program, resulting in a partial EMT state [79], which is distinguished by the simultaneous presence of both epithelial and mesenchymal traits, enabling a more efficient collective cell migration and invasion [80]. This stiffness-induced hybrid EMT state can be regulated at least in part by the transcription factor Twist1 [79]. In soft environments, Twist1 remains cytoplasmic by binding to Ras GTPase-activating protein-binding protein 2 (G3BP2) [79]. However, matrix stiffening promotes the dissociation of the Twist1-G3BP2 complex, and the translocation of Twist1 to the nucleus, where it initiates EMT, thereby promoting breast tumor invasion and metastasis [79]. In addition, breast cancer cells that express the EMT transcription factors Twist1, Snail1, and Six1 can enhance the migratory and metastatic potential of neighboring, non EMT tumor cells by activating the GLI-induced transcription factor in a non-cell autonomous manner [81].

**Table 3** Comparative stiffness analysis between healthy and abnormal human breast tissues

Breast Tissue	Elastic modulus	Stiffness (kPa)
Normal Breast Parenchyma	Young's modulus	$31.3 \pm 1.6^d$ [104] $0.4^c$ [75]
Benign conditions	Young's modulus	$34.8 \pm 17.7^a$ [105]
	Shear modulus	$0.87 \pm 0.15^b$ [106] $1.4 \pm 0.5^b$ [107]
Breast Carcinoma	Young's Modulus	$140.7 \pm 58.5^a$ [105]
	Non-invasive	$42.8^a$ [108]
	Invasive ductal	$174.4 \pm 42^a$ [108] $\sim 3^c$ (invasive front) [75]
Luminal breast cancer	Shear modulus	$208.2^a$ [108]
	Young's Modulus	$136.9 \pm 57.2^a$ [109] $91.4 \pm 30.7^a$ (Luminal A) [110] $108.2 \pm 27.1^a$ (Luminal B) [110]
	Young's Modulus	$118.0 \pm 32.1^a$ [110] $160.3 \pm 56.2^a$ [109]
HER2 positive breast cancer	Young's Modulus	$118.5 \pm 30.8^a$ [110]
	Young's Modulus	$165.8 \pm 48.5^a$ [109]

<sup>a</sup>Shear wave elastography, <sup>b</sup> Magnetic resonance elastography, <sup>c</sup>Atomic force microscopy, <sup>d</sup>Virtual touch tissue imaging quantification

Cells perceive elevated stiffness primarily through integrins, which promote cell spreading and Ras homolog family member A (RhoA)-dependent cytoskeleton tension [82–85, 77]. As a result, increased stiffness triggers the translocation of the transcription factor co-activators Yes-associated protein (YAP) and transcriptional coactivator with PDZ-binding motif (TAZ) to the nucleus where they interact with the transcriptional enhanced associate domain (TEAD) family of transcription factors to induce gene expression [85]. In contrast, low stiffness increases the activity of the Ras-related GTPase RAP2 which inactivates RhoA and induces the phosphorylation of the large tumor suppressor kinase 1/2 (LATS1/2). In turn, LATS1/2 phosphorylate YAP/TAZ to inactivate them, promoting their cytoplasmic localization [86].

Elevated YAP nuclear levels have been detected in CAFs within adenoma and carcinoma lesions in mice as well as in stromal fibroblasts of human breast cancer. Interventions aimed at reducing YAP levels or increasing their activity in CAFs provide evidence that YAP is essential for CAFs-dependent tumor cell invasion, matrix stiffening, and angiogenesis [87]. Interestingly, in contrast to CAFs, YAP nuclear intensity exhibits a significant decrease in both ductal carcinoma *in situ* and in invasive ductal carcinomas [88, 89]. This decrease is likely attributed to the loss of stress fibers and the reduction of nuclear area, which are observed in 3D environments but not on 2D surfaces [89]. The loss of YAP in breast cancer leads to increased tumor cell invasion, proliferation, resistance to chemotherapeutics, and protection against cell death, suggesting that YAP acts as a tumor suppressor [88].

Matrix stiffness has been shown to strongly influence the migration of breast cancer cells. Experiments conducted using a polyacrylamide-based microchannel device that allows independent control of substrate stiffness and channel dimensions revealed that optimal migration of triple-negative MDA-MB-231 and SUM159 human breast cancer cells occurs at intermediate stiffness [90]. This biphasic stiffness dependence finds its explanation in the motor-clutch model. According to this model, myosin motors, actin cytoskeleton, and cell adhesion molecules like integrins (clutches) cooperate and coordinate to facilitate cell migration [91–93]. The motor-clutch model predicts that cells generate maximal traction force at intermediate stiffness [92]. Moreover, it demonstrates that a change in the number of motors and clutches can alter the optimal stiffness for cell migration [93]. While these predictions have been experimentally confirmed [93], it has been observed that the optimal stiffness is often masked because, beyond a certain stiffness threshold, talin mediates adhesion reinforcement, leading to an increase in cell traction [94].

Substrate stiffness can also act as a guiding cue for migrating tumor cells. Research indicates that cells respond to stiffness gradients through a process called durotaxis (from Latin “durus” meaning hard and Greek “taxis” meaning arrangement), initially observed using fibroblasts [82]. While certain tumor cells, like MDA-MB-231 cells, display positive durotaxis by moving from soft (0.5 kPa), to stiff (22 kPa) substrates [95, 96], others, such as U-251MG glioblastoma brain tumor cells, undergo negative durotaxis, migrating from 22 kPa regions towards softer, 10 kPa, areas [96]. Recent work has significantly advanced our understanding of the intricate mechanisms that govern these diverse durotactic responses. By employing a combination of experimental and computational approaches, the Odde lab demonstrated that cells preferentially move toward areas of optimal stiffness, where they produce maximum traction forces [96]. For U-251MG cells, this optimal stiffness has been found to be ~10 kPa, while for MDA-MB-231 cells, it is ~20 kPa. Interestingly, negative durotaxis of U-251MG cells can be reversed by a partial reduction in myosin motors which increases the optimal stiffness of these cells. On the other hand, talin knockdown promotes negative durotaxis of MDA-MB-231 cells by suppressing adhesion reinforcement, which is observed on ~20 kPa substrates [96].

Therapeutic approaches aimed at targeting CAFs and their products show promise in suppressing breast tumor progression. Attractive targets include members of the LOX family, namely LOX and LOX-like 2 (LOXL2), which mediate collagen and/or elastin crosslinking [97, 98], thereby contributing to ECM remodeling in the tumor microenvironment. Chemical inhibition of LOX activity using β-Aminopropionitrile (BAPN) has been shown to increase tumor latency and decrease tumor incidence in the mouse mammary tumor virus (MMTV)-Neu model [70]. BAPN also re-sensitizes triple-negative breast cancer cells to chemotherapy as seen in different triple-negative breast cancer models, including chemoresistant xenografts, syngeneic tumors and PDX models [99]. Moreover, in a xenograft mammary 4T1 tumor model, it has been demonstrated that the concurrent administration of BAPN and the enzyme-responsive drug (NQO1-SN38), designed to target breast tumors with the topoisomerase I inhibitor SN38, results in a cooperative reduction in tumor growth [100]. The copper chelator tetrathiomolybdate, which blocks the copper-dependent catalytic activity of LOX, is presently undergoing a phase II study (NCT00195091) involving patients with breast cancer at moderate to high risk of recurrence. Furthermore, chemical or genetic inhibition of LOXL2 significantly reduces metastasis in orthotopic and transgenic breast cancer models [101]. Elevated LOXL2 expression in estrogen receptor-negative breast tumors is strongly associated with unfavorable outcomes, including poor prognosis,

decreased overall survival, and reduced metastasis-free survival, suggesting that LOXL2 could serve as a valuable prognostic marker for metastasis in breast cancer cases. The antibody simtuzumab, targeting extracellular LOXL2, has undergone clinical trials in combination with gemcitabine for patients with metastatic pancreatic adenocarcinoma or with FOLFIRI (folinic acid, fluorouracil, and irinotecan) for patients with KRAS mutant colorectal cancer [102, 103]. However, the addition of these chemotherapeutics does not yield improved clinical outcomes, presumably because simtuzumab exclusively inhibits extracellular LOXL2. Phase I and phase II trials are also underway to assess the safety and pharmacokinetics of small molecule inhibitors of LOXL2, such as GB2064 (NCT04679870) and PXS-5382 A (NCT04183517). It is noteworthy that as of now, these inhibitors have not been tested for breast cancer treatment.

#### 4 Solid stress: compressive and residual stress

Breast cancer growth as well as collagen and hyaluronan deposition within the confined tissue environment results in the buildup of mechanical stress (aka solid stress) within tumors. This stress squeezes lymphatic and blood vessels, elevating IFP, hindering the effective delivery of chemotherapeutics, and promoting hypoxia [111, 112]. Two primary factors contribute to solid stress: compressive and residual stress [111, 113–115]. Compressive stress arises from the surrounding healthy tissue as it counteracts tumor growth. Residual stress is generated from intratumoral cell-cell, cell-ECM interactions, and consequently, persists even after tumor excision [115]. In human breast tumors, this stress is estimated to range from 10 to 19 kPa [115]. Although ultrasoundography has enabled the *in situ* evaluation of 1D profile of solid stresses within glioblastoma tumors [111], the estimation of both the isotropic and anisotropic components of the stress tensor exerted on cells and tissues remained elusive until recently. This has been addressed through the use of multimodal intravital microscopy of deformable and adjustable in size fluorescently-labelled polyacrylamide beads that allow spatiotemporal measurements of solid stress applied to relatively small animal tumors *in vivo* [116]. This innovative technique has revealed that the solid stress imposed on murine breast tumors is ~2 kPa, a magnitude 5 to 8 times higher than the stress that individual cancer cells sense within the primary tumor [116]. Intriguingly, breast cancer cells in metastatic lung tumors experience higher magnitude of solid stress compared to those in the primary tumor, underscoring the key role of the local microenvironment in modulating solid stress during cancer progression [116]. Despite the significance of this method

in measuring solid stress *in vivo*, its clinical applicability is hindered by the need for intravital window implantation.

In vitro and *in vivo* studies have provided valuable insights into how compressive stress affects breast cancer cell behavior. Initial studies using cancer cells embedded in non-degradable agarose gels showed that compressive stress exerted by the confining matrix on the mammary tumor spheroids suppresses proliferation and survival [117, 118]. However, more recently, it has been shown that tumor cells, including MDA-MB-231 and MCF7 breast cancer cells, display increased proliferation when subjected to confining stress from stiff (>30 kPa), degradable, 3D, hyaluronan-based gels, compared to softer (~4 kPa) hydrogels [119]. These stiff gels activate the mechanosensitive ion channel (MIC) TRPV4, which upregulates the activity of the phatidylinositol 3-kinase(PI3k)/Akt pathway, triggering the expression of heat shock protein-(HSP-) 70, which protects against stress-induced cell death [119]. Moreover, HSP-70 enhances tumorigenicity and metastasis in murine models and promotes the expression of stemness markers (Nanog, Oct3/4, and SOX2) in stiff hydrogels by increasing the activity of the transcription factor signal transducer and activator of transcription 3 (STAT3) [119]. The disparity in findings across studies could stem from the characteristics of the hydrogel system used, such as its degradability and its initial stiffness. Additionally, differences in cell lines (e.g., P53 status) could lead to divergent cell responses to solid stress.

Furthermore, the application of external compressive stress of 0.77 kPa has yielded diverse migratory responses in breast cancer cells. While highly aggressive triple-negative 4T1 and MDA-MB-231 breast cancer cells show increased migration under this stress, non-metastatic, luminal A MCF7 breast cancer cells experience a significant reduction in motility [120]. Compression-induced invasion and migration of breast cancer cells are attributed to the activation of the MIC Piezo 1 [121] and the formation of leader cells, which possess filopodia at their leading-edge, thereby driving persistent and directional motility [120]. Interestingly, the application of low-magnitude compressive stress (0.03 kPa) on weakly adhesive MDA-MB-231 breast cancer cells decreases their motility, highlighting the critical role of cell-matrix interactions in stress-dependent cell responses [122].

Besides its role in regulating cell division, viability, and motility, compressive forces can also influence gene expression [123]. Compression- or actomyosin-mediated nuclear flattening alters the permeability across nuclear pore complexes, resulting in active nuclear import of key transcription regulators such as YAP, SMAD3, Twist1, and Snail [124, 125]. Compressive stress also induces promoter hypermethylation of microRNA-9 (miR-9) precursors, leading to

miR-9 downregulation, which increases VEGFA expression [126]. This mechanism, which is observed in breast CAFs, as well as in luminal B (BT-474) and triple-negative (MDA-MB-231) breast cancer cells, but not in HER2 (SK-BR-3) and luminal A (MCF7) tumor cells, may contribute to angiogenesis in breast tumors [126].

Interventions aimed at blocking collagen and hyaluronan production, such as a neutralizing antibody against TGF- $\beta$  [127], the angiotensin inhibitor losartan [128–131], or the antifibrotic drugs tranilast and pirfenidone [132–134] have shown promising results in alleviating solid stress and increasing breast tumor blood supply and drug delivery. As a result, these interventions boost the efficacy of chemotherapeutic agents, markedly suppressing breast tumor growth in preclinical animal models of breast cancer [127–132, 134]. Importantly, a clinical study has demonstrated that combining radiotherapy with higher doses of the TGF $\beta$ -blocking antibody fresolimumab (10 mg/kg) increases overall survival significantly in metastatic breast cancer patients compared to those undergoing radiotherapy and receiving lower doses of fresolimumab (1 mg/kg) [135]. Furthermore, in a phase II study, the combination of chemotherapy (albumin-bound paclitaxel and gemcitabine) along with pegvorhyaluronidase alfa (PEGPH20), an agent designed to degrade hyaluronan, has been shown to improve progression-free survival in pancreatic cancer patients, especially those with hyaluronan-high tumors [136]. However, the potential efficacy of such approach for breast cancer patients remains to be determined.

## 5 Viscoelasticity

Various living tissues and natural ECMs exhibit both viscous (fluid-like) and elastic (spring-like) behavior. While purely elastic materials recover their shape following stress application, viscoelastic materials display (a) a time-dependent stress decrease in response to a constant strain (aka stress relaxation), (b) a time-dependent strain increase under constant stress (aka creep), and (c) an energy dissipation and a delayed response as the materials undergo loading and unloading (aka hysteresis) [137]. Stress relaxation tests have revealed that the time it takes for biological tissues to relax to half the magnitude of the initially applied stress varies significantly. For instance, the relaxation time can range from seconds in the brain, to minutes in the liver, and hours in the skin, with faster stress relaxation indicating increased viscoelasticity [138]. Although the investigation of the role of viscoelasticity in health and disease has recently just begun, techniques such as shear wave elastography, and magnetic resonance elastography have demonstrated that malignant breast tumors exhibit more viscoelastic behavior

relative to benign and normal tissues [139–141]. Moreover, the indentation method has revealed that human breast tumors exhibit stress relaxation half time of ~10 s [142].

The Chaudhuri lab investigated the effects of viscoelasticity on tumor cell behavior using alginate gels with varying stress relaxation times. They found that the 2D motility of HT-1080 fibrosarcoma cells, MDA-MB-231 breast cancer cells, and normal breast epithelial MCF-10 A cells is faster on fast- (~100 s) relative to slow-relaxing (~2,000 s), soft (2 kPa) substrates [143]. This effect is attributed to the increased formation of nascent adhesions and filopodia at the cell periphery and cell front, respectively [143]. In addition to promoting cell migration, fast- (~60 s) but not slow- (~6,000 s) relaxing hydrogels allow breast cancer cells to grow in size and divide in 3D confining environments. Cell growth, controlled by sodium-hydrogen ion exchangers (NHEs), induces MIC-dependent activation of the PI3K/Akt pathway, which in turn supports the cytoplasmic localization of the cell cycle inhibitor p27<sup>Kip1</sup>, resulting in tumor cell proliferation [142]. Furthermore, measurements have shown that human breast tumors display plastic deformation (i.e., permanent deformation when subjected to external forces) [144], likely due to the increased collagen concentration and crosslinking observed in the breast tumor microenvironment which can enhance plasticity [145]. To model this plastic behavior, 3D hydrogels composed of reconstituted basement membrane and alginate are used. Increased plasticity has been shown to facilitate protease-independent migration of breast cancer cells by promoting the formation of invadopodia protrusions, which in turn generate contractile forces to create migratory paths for the cells [144].

## 6 Cellular confinement

Microscopy techniques, including intravital microscopy, have revealed that metastatic cancer cells traverse microenvironments that impose different levels of confinement on cells. Examples of such environments are microvessels with diameters smaller than the size of tumor cells [146], narrow (~1–5  $\mu\text{m}$ -sized) gaps between endothelial cells [147], micropores with diameters ranging from 1 to 20  $\mu\text{m}$  [148], ECM fibers [149], and longitudinal, channel-like tracks with widths ranging from 3 to 30  $\mu\text{m}$  [150]. Advances in patterning, materials and microfabrication techniques have enabled researchers to isolate and investigate the effects of confinement on tumor cell behavior. In vitro models to study confinement-induced responses include micropatterned lines [151], 2D micropatterned substrates [85], uni-axial compression [152], polydimethylsiloxane [153–156]- or polyacrylamide [90]-based microchannel devices, microniches [157, 158], and natural hydrogels [148, 159]. These versatile

tools enable in-depth studies of cellular responses to 1D, 2D or 3D confinement [85, 148, 152, 159, 160], moderate or tight confinement [157, 158, 153–155, 160], short- or long-term confinement [153–155, 160], and confining pores or channels [148, 159, 153–155]. Additionally, recent research has delved into the interplay between confinement and other physical cues (e.g., stiffness [90], viscoelasticity [142], and viscosity [161]) in relation to cancer cells, revealing their combined contributions to different cell processes.

It is well established that breast cancer cells alter their migration modes and mechanisms to adapt to 3D confinement. Inhibition of key regulators of 2D cell locomotion such as actin polymerization, cell-matrix adhesion, and myosin contractility fail to block confined migration of MDA-MB-231 breast cancer cells [153], suggesting the existence of alternative mechanisms facilitating their movement. The Osmotic Engine Model (OEM) predicts that confined cell migration is facilitated by directed water permeation driven by a gradient of aquaporins, ion transporters, and ion channels [162]. Consistent with the OEM, experiments have demonstrated that in confinement, aquaporin 5 and the sodium-hydrogen exchanger 1 (NHE1) localize at the cell front, promoting isosmotic cell swelling [162]. On the other hand, aquaporin 4 and the SWELL1 chloride channel (LRRC8A) accumulate at the cell rear mediating cell shrinkage [163]. Dual depletion of NHE1 and SWELL1 markedly suppresses breast cancer cell migration, extravasation, and metastasis, underscoring the pivotal role of this migration mechanism in breast cancer progression [163]. Furthermore, while in 2D/unconfined environments breast cancer cells maintain a mesenchymal migration phenotype characterized by actin-rich protrusions and adhesion to the substrate [7], in confinement, cells switch to an amoeboid/bleb-based migration mode [152, 164, 165]. Amoeboid cells exhibit weak adhesions, show high dependence on actomyosin contractility, and utilize spherical bulges known as membrane blebs for efficient migration, invasion, and extravasation [166–168]. Amoeboid-based migration of breast cancer cells has been found to correlate with lymph node metastasis [169].

Tumor cell migration speed scales with pore size in 3D hydrogels. However, in the absence of matrix degradation, pore sizes smaller than  $7 \mu\text{m}^2$  impede cellular locomotion because the nucleus, which is the stiffest and largest cell organelle, acts as a rate-limiting barrier to migration [170–172]. Consistent with these findings, migration studies conducted in confining microenvironments have demonstrated an inverse correlation between nuclear rigidity or nuclear volume expansion with migration efficiency [173–177]. The nuclear lamina, which lines the inner surface of the nuclear envelope, is the main determinant of nuclear stiffness, providing structural support to the nucleus. It is

composed of A- (A, C, C2) and B- (B1, B2, B3) type lamins, a mesh-like network of intermediate filament proteins [175, 178, 179]. Lower levels of lamin-A induced by the PI3K/Akt pathway facilitate nuclear deformation in confinement, support breast cancer cell invasion and associate with reduced disease-free survival [174]. B-type lamins can also enhance nuclear stiffness, thereby impacting confined migration [180, 181]. Other factors contributing to nuclear rigidity include the chromatin organization [182] and the LINC (Linker of Nucleoskeleton and Cytoskeleton) complex [183]. It is worth noting, that in addition to nuclear stiffness, A-and B-type lamins regulate other hallmarks of cancer, including cell proliferation and chromatin organization [184–186], underscoring their multifaceted role in tumor progression. Importantly, high lamin-B1 has been found to predict unfavorable outcomes in patients with different types of cancer [187].

Confinement exerts stress on the nucleus, triggering the formation of nuclear protrusions (aka nuclear blebs), which lack lamin B1 and nuclear pores and lead to transient ruptures of the nuclear envelope [188–190]. Actomyosin contractility can compromise nuclear integrity by squeezing the nucleus dorsoventrally [191, 192], pulling it [193] or promoting the nuclear influx of cytoplasmic constituents, which in turn pressurizes the nucleus, leading to its rupture [155]. Seminal studies have demonstrated that nuclear ruptures occur at sites characterized by pronounced curvature [194], leading to DNA damage and genomic instability [188–190]. These adverse effects stem from the entry of the cytoplasmic exonuclease TREX1 into the nucleus, which induces DNA cleavage [195], as well as the translocation of DNA repair factors such as Ku70, Ku80, and BRCA1 to the cytoplasm [190, 194]. Nuclear deformation can promote DNA damage even without instances of nuclear envelope ruptures. This type of DNA damage is more evident in MDA-MB-231 or BT-549 breast cancer cells, manifesting at replication forks and causing replication stress [196]. Although confinement suppresses MDA-MB-231 cell proliferation [160], it proves ineffective in inducing death in these cells as they harbor mutations in the gene encoding P53 [160]. P53 mutations are highly prevalent in breast tumors [197] potentially granting a survival advantage to breast cancer cells as they navigate mechanically challenging microenvironments.

Accumulating evidence suggests that tumor cell exposure to confinement can promote breast cancer progression. The invasive front of confined breast tumors exhibits pronounced nuclear deformation, nuclear rupture, and DNA damage [195]. A key player in the formation of invasive breast tumors is TREX1, which mediates confinement-induced DNA damage, collagen degradation, and the acquisition of a hybrid epithelial-mesenchymal phenotype [195]. Additionally, confinement triggers resistance

to chemotherapeutics [198] and to programmed cell death triggered by loss of adhesion (aka anoikis) [199] which in turn facilitates breast cancer metastasis [199]. Collectively, confinement is a pathophysiologically relevant cue that can influence tumor progression significantly by altering the modes and mechanisms of cancer cell migration, promoting genomic instability, and inducing gene expression changes, which trigger EMT and provide resistance to therapeutic agents.

## 7 Hydraulic resistance

Tumor cells migrate through confining, water impermeable channels by generating pressure at their leading-edge ( $P_{LE}$ ), which enables them to push the column of fluid ahead of them (Fig. 2). Assuming that cells are impermeable to water,  $P_{LE}=P_1 + \langle v \rangle AR$ , where  $P_1$  is the upstream pressure (Fig. 2),  $\langle v \rangle$  is the average fluid/cell velocity (since the fluid moves at the same speed as the cell), A is the cross-sectional area and R is the hydraulic resistance (i.e., the external load that resists cell/fluid movement) which, for rectangular channels, is proportional to the channel length L. This equation implies that if  $\langle v \rangle$ ,  $P_1$  and A are constant, it becomes easier for cells to migrate through channels with lower resistance, as they would need to generate less  $P_{LE}$ . Indeed, when neutrophil-like cells (HL-60 cells) encounter channels with varying levels of hydraulic resistance, they preferentially select the path of least resistance. Intriguingly, when the hydraulic resistance is infinite, nearly all cells move towards the lower hydraulic resistance geometries [200].

MDA-MB-231 breast cancer cells, much like immune cells, demonstrate a preference for low resistance channels [50]. Using trifurcating  $\Psi$ -like microchannels, the Konstantopoulos lab studied how tumor cells respond to channels with different resistances. Their research revealed that the branch channel with the higher resistance triggers the TRPM7-mediated influx of  $\text{Ca}^{2+}$ , resulting in the local formation of a thicker cortical actin network enriched with elevated levels of myosin II-A. This increase in actomyosin contractility guides cells towards low resistance channels [50]. Tumor cell migration along the path of least resistance is energetically favorable [201]. However, increasing cell compliance or reducing matrix stiffness suppresses energetic costs, blinding MDA-MB-231 cells to hydraulic resistance and enabling them to navigate through high-resistance

migratory paths that would otherwise demand more energy [201]. Hydraulic resistance also alters the migration phenotype of confined MDA-MB-231 cells [202], by inducing the transition from an amoeboid phenotype to a mesenchymal phenotype [202]. This switch is controlled by TRPM7-dependent  $\text{Ca}^{2+}$  influx and requires actin polymerization, myosin recruitment and the formation of focal adhesions at the interface between the cell and the lateral channel walls. This redistribution of actomyosin contractility decreases cortical contractility, promoting amoeboid to mesenchymal transition [202]. Although the magnitude of hydraulic resistance experienced by migrating breast cancer cells *in vivo* is currently unknown, mathematical modeling indicates that depending on the interstitial fluid viscosity and matrix permeability, the hydraulic resistance within 3D matrices could potentially match or even exceed that observed in microchannels [50, 203]. This suggests that hydraulic resistance could significantly impact cell migration and decision-making *in vivo*.

## 8 Extracellular fluid viscosity

In basic cell culture, the medium typically used matches the viscosity of water (~0.7 cP at 37 °C). However, *in vivo*, the viscosity of extracellular fluids is higher than 0.7 cP (Table 4). Extracellular fluid viscosity is further elevated in tumors as recently demonstrated in a study that employed new viscosity-sensitive fluorescent probes for noninvasive imaging of murine breast tumors [204]. Shear wave elastography also showed that malignant breast tumors display a shear viscosity ~3 times higher than benign tumors and ~6 times higher than normal breast tissue (8.22 Pa·s, 2.83 Pa·s, 1.41 Pa·s, respectively) [140]. This increase in extracellular viscosity can be attributed to the accumulation of ECM degradation products [205] or macromolecules (e.g., Mucins [206]) caused by the collapse of the lymphatic drainage system [17, 18]. Furthermore, clinical studies have shown that increased plasma viscosity correlates with poor survival in breast cancer patients [207]. Despite these findings, the impact of fluid viscosity on breast cancer progression remains largely unexplored. Recent work has shown that elevated viscosity increases the migration of both cancerous and non-cancerous cells [161, 208, 209]. This finding is counterintuitive, as higher viscosity is known to suppress the movement of particles in fluids.

**Table 4** Viscosity measurements of different extracellular fluids

Extracellular Fluid	Range of viscosity (cP)	Range of shear rates ( $\text{s}^{-1}$ )	Fluid behavior
Synovial fluid	~70–900 [210]	10–250 [210]	Shear thinning
Cerebrospinal fluid	~0.7–1 [211]	25–1,460 [211]	~Newtonian
Gastric mucus	~500–7,000 [212]	1.15–46 [212]	Shear thinning
Blood	~3–5 [213]	1–100 [213]	Shear thinning

Cells sense elevated viscosity through their actin cytoskeleton, which rapidly reorganizes into a dense network that polarizes and activates NHE1 [161]. In turn, NHE1 promotes cell volume expansion, which increases membrane tension, resulting in TRPV4-mediated calcium influx and the activation of actomyosin contractility [161]. Moreover, elevated viscosity suppresses membrane ruffling, allowing the cell membrane to stay adjacent to the substrate, thus increasing integrin-substrate engagement [208]. These viscosity sensing mechanisms enhance cell traction force, promote cell spreading, and allow breast cancer cells to migrate faster on 2D substrates and in confining microchannels [161, 208]. Furthermore, breast cancer cells develop YAP-dependent viscous memory that enhances their migration in zebrafish, extravasation in chick embryos and lung metastasis in mice [161]. These studies suggest that the elevated extracellular fluid viscosity within breast tumors triggers cancer cell invasion and metastasis. However, it remains unclear how this physical signal affects other hallmarks of cancer, including drug resistance and angiogenesis.

## 9 Drag forces: shear and pressure drag

Pressure gradients are highly prevalent within the human body, serving as the driving force behind fluid flow, including transmural, interstitial and blood flow. Moving bodily fluids display significant disparities in velocities, often differing by several orders of magnitude. Techniques such as fluorescence recovery after photobleaching and dynamic contrast-enhanced magnetic resonance imaging (MRI) have demonstrated that interstitial fluid generally moves at a relatively slow velocity, ranging from 0.1 to 10  $\mu\text{m}/\text{s}$ , depending on the species under consideration [214]. In the context of cancer, the pressure buildup within the tumor relative to the surrounding tissue leads to a notable increase in interstitial flow, typically by 3–5 times [215]. Blood flow is much faster, reaching speeds of several  $\text{mm}/\text{s}$  in capillaries or  $\text{cm}/\text{s}$  in veins and arteries [216–218].

Moving fluid is known to exert drag forces on tumor cells in the direction of flow due to the combined effects of shear and pressure forces. While shear forces act tangentially to the cell's surface, pressure drag acts normal to it. The shear stress, representing shear force per unit area, is particularly elevated near the vessel wall with values ranging from 1 to 4  $\text{dyn}/\text{cm}^2$  in veins, and 4–30  $\text{dyn}/\text{cm}^2$  in arteries [219]. As cells attempt to invade a blood vessel, they encounter shear forces acting on them. The diminished shear sensitivity of tumor cells like MDA-MB-231 cells or HT-1080 fibrosarcoma cells allows them to enter high-shear environments [220]. However, ectopic expression of TRPM7 restores their shear sensitivity, leading to a marked

reduction in intravasation and metastatic lesion formation [220]. TRPM7 elicits its effects by triggering  $\text{Ca}^{2+}$  influx in response to fluid shear, thereby activating RhoA-dependent contractility and the calmodulin/IQGAP1/Cdc42 pathway [220]. This shear-sensing mechanism allows cells to reverse their migration direction, effectively avoiding entry into high-shear environments [220].

The increased shear stress in the circulatory system can pose a threat to circulating tumor cells (CTCs), triggering apoptosis or necrosis [221, 222]. Although breast cancer cell lines exhibit increased resilience to physiologically relevant shear stress compared to normal epithelial cells [223], lamin A/C knockdown exacerbates shear stress-mediated tumor cell death [223], suggesting that elevated lamin A/C levels could aid breast CTCs in withstanding shear forces in the circulation. CTCs that survive the harsh conditions induced by elevated shear stress acquire stem cell-like properties and display a mesenchymal phenotype [224, 225]. These shear stress-induced changes involve the activation of Jun N-terminal kinase (JNK) signaling and the downregulation of extracellular signal-related kinase (ERK) and glycogen synthase kinase (GSK)3 $\beta$  [224, 225].

The impact of shear stress on cell migration varies depending on the specific breast cancer cell line. Highly invasive triple-negative MDA-MB-231 cells respond to 15  $\text{dyn}/\text{cm}^2$  by increasing their migration velocity, whereas normal MCF-10 A epithelial cells and less aggressive triple-negative MDA-MB-468 breast cancer cells show only slight or no increase in motility under the same conditions, respectively [226]. MDA-MB-231 cells even respond to lower shear stress values (1.8  $\text{dyn}/\text{cm}^2$ ) by adhering more to the substrate and reorienting the Golgi marker GM130 in the direction of flow [227]. Shear stress regulates breast cancer cell adhesion to endothelial cells. Optimal tumor cell adhesion is observed under low flow conditions, typically encountered in the venous but not arterial system [228, 229]. However, efficient extravasation also requires remodeling of the endothelium, a process that occurs at higher blood flow velocities and involves the engulfment of tumor cells by endothelial cells [229]. Thus, an optimal flow velocity range of 400–600  $\mu\text{m}/\text{s}$  has been found to favor both tumor cell arrest within vascular regions and endothelial remodeling, leading to extravasation and metastasis [229].

While the effects of shear forces on tumor cell behavior are well-established, the impact of pressure drag on these cells remains largely unexplored. Computational fluid dynamics simulations have revealed that the pore size within a 3D matrix governs the relative magnitude of shear and pressure drag acting on a cell [230]. These simulations indicate that within highly confined matrices, such as those encountered *in vivo*, the force resulting from the pressure drop across the cell dominates over the total shear force

**Table 5** Influence of physical cues on tumor progression

Physical cue	Mechanosensing mechanisms and their impact on tumor progression
IFP	<ul style="list-style-type: none"> <li>- Activates TRPM7, leading to calcium influx and thicker actomyosin cortex [50]</li> <li>- Upregulates aquaporin 1 to enhance tumor cell migration [52]</li> <li>- Regulates cancer cell proliferation [51]</li> <li>- Triggers ABCC1-dependent drug resistance [53]</li> </ul>
ECM stiffness	<ul style="list-style-type: none"> <li>- Promotes MMP-mediated angiogenesis and increases vascular permeability [76]</li> <li>- Triggers focal adhesion formation, increases Rho activity and promotes tumor progression [77]</li> <li>- Upregulates integrin-linked kinase (ILK) to induce cancer stem cell development [78]</li> <li>- Regulates the TWIST1-G3BP2 pathway to initiate EMT, invasion and metastasis [79]</li> <li>- Controls tumor cell migration efficiency and direction [90, 96]</li> <li>- Induces YAP translocation to the nucleus which mediates the pro-tumorigenic functions of CAFs [85, 87]</li> </ul>
Solid stress	<ul style="list-style-type: none"> <li>- Regulates tumor growth and survival [117–119]</li> <li>- Activates Piezo 1 and the TRPV4-PI3K/Akt pathway [119, 121]</li> <li>- Upregulates HSP-70 to promote stemness, cancer cell survival and metastasis [119]</li> <li>- Regulates cancer cell migration [120]</li> <li>- Induces VEGFA expression [126]</li> <li>- Regulates active and passive nucleocytoplasmic transport [124, 125]</li> </ul>
Viscoelasticity	<ul style="list-style-type: none"> <li>- Increases tumor cell migration on soft substrates [143]</li> <li>- Promotes the formation of nascent adhesions and filopodia protrusions on soft substrates [143]</li> <li>- Enables tumor cell proliferation in 3D environments [142]</li> <li>- Activates MICs which control the PI3K/Akt-p27 pathway [142]</li> </ul>
Cellular confinement	<ul style="list-style-type: none"> <li>- Polarizes aquaporins, ion channels and ion transporters which facilitate cancer cell migration, extravasation and metastasis [162, 163]</li> <li>- Triggers nuclear envelop rupture, nuclear-cytoplasmic exchange of material and DNA damage [188–190]</li> <li>- Activates P53-dependent DNA damage responses [160]</li> <li>- Suppresses YAP activity [160]</li> <li>- Reduces proliferation [160]</li> <li>- Promotes the transition from a mesenchymal to an amoeboid phenotype [152, 164, 165]</li> <li>- Triggers resistance to chemotherapeutics [198]</li> <li>- Induces resistance to anoikis [199]</li> <li>- Promotes cancer cell invasion and metastasis [195, 199]</li> </ul>
Hydraulic resistance	<ul style="list-style-type: none"> <li>- Activates TRPM7 [50]</li> <li>- Influences tumor cell decision making in confinement [50, 201]</li> <li>- Promotes the transition from an amoeboid to a mesenchymal phenotype [202]</li> </ul>
Viscosity	<ul style="list-style-type: none"> <li>- Induces actin remodelling which activates the NHE1-TRPV4-RHOA-Myosin II pathway [161]</li> <li>- Suppresses membrane ruffling [208]</li> <li>- Promotes cancer cell invasion, migration, extravasation and metastasis [161, 208, 209]</li> </ul>
Drag forces	<ul style="list-style-type: none"> <li>- Activate TRPM7-RhoA-Myosin II and calmodulin-IQGAP1-Cdc42 pathways [220]</li> <li>- Control cancer cell intravasation [220]</li> <li>- Activate JNK signaling and suppress ERK-GSK3β [224, 225]</li> <li>- Compromise cell survival [221, 222]</li> <li>- Regulate tumor cell adhesion to the endothelium and extravasation [228, 229]</li> <li>- Control migration direction [231, 232]</li> <li>- Upregulate mesenchymal and epithelial genes [237]</li> <li>- Promote the amoeboid mode of migration [238]</li> </ul>

[230]. Hence, in these microenvironments, pressure drag accounts for the majority of the total drag experienced by the cell. By employing 3D hydrogels typically characterized by small, micron-sized pores, the Kamm and Swartz labs have shown that (patho)physiologically relevant flow velocities can trigger migration of MDA-MB-231 in the upstream (against the flow) and downstream (with the flow) direction [231, 232]. Downstream migration is mediated by self-secreted ligands, specifically CCL19 and CCL21, which bind to the chemokine receptor CCR7 [233]. These ligands are distributed downstream due to convective flow, resulting in an autologous chemotaxis mechanism, which can direct tumor cells towards the draining lymphatics, facilitating

their metastatic spread [233]. In contrast, upstream migration of tumor cells is regulated by focal adhesions, which polarize at the upstream side of the cell [234]. Cell migration against the flow can be observed in high-density cultures [234]. This behavior is consistent with results obtained from densely seeded suspensions of MDA-MB-231 cells in collagen gels, where cells tend to stay in high-pressure environments and do not move with the flow [235, 236]. These intriguing findings imply that the elevated IFP within the tumor may act as an anti-metastatic signal, hindering tumor cell escape. Furthermore, flow conditions that promote invasion of MDA-MB-231 aggregates in collagen gels trigger the upregulation of mesenchymal (Vimentin

and Snail1) and epithelial (E-Cadherin and keratin-8) genes [237]. Depletion of Vimentin nearly abolishes flow-induced invasion [237]. MDA-MB-231 cells also undergo phenotypic transitions in 3D hydrogels under the influence of physiologically relevant flows. While in the absence of flow, cells migrate using a mesenchymal phenotype, cell exposure to flow promotes a faster amoeboid-based migration [238]. Collectively, these findings highlight the significant influence of pressure-driven flow fields on various aspects of breast cancer progression.

## 10 Conclusions and future directions

While the existence of physical stimuli within the breast tumor microenvironment and throughout the metastatic cascade has been acknowledged for several decades, our understanding of their role in breast cancer remains incomplete. Recent advances in bioengineering have provided powerful tools to tune biophysical and topographical cues of the microenvironment, opening up new avenues to explore how these signals contribute to tumor progression. However, these techniques often permit the investigation of only one factor at a time, hindering our ability to unveil the intricate interplay of various physical factors in cancer. Furthermore, little is known about the role of physical signals in the progression of different breast cancer molecular subtypes. Tailoring treatments according to the distinct features of the breast tumor microenvironment and its interactions with different molecular subtypes of breast cancer may facilitate the development of personalized medicine approaches.

Although a plethora of tumor cell mechanosensors have been identified, including focal adhesions, ion channels, actin cytoskeleton, nuclear proteins, and transcription factors, more research is needed to uncover how breast cancer cells convert biophysical signals into biochemical cues to mediate short- and long-term mechanoresponses (Table 5). Gaining a deeper understanding of the crosstalk between different mechanosensors may inspire the development of new therapeutic strategies to block tumor progression. To date, the focus of new drug development and therapies has primarily revolved around targeting tumor growth, often overlooking metastatic spread, which accounts for the vast majority of breast cancer-associated deaths. Given the established role of confined cell migration in breast cancer metastasis [239], it is critical to identify interventions that can target and modulate cell motility.

Physical signals hold significant potential as valuable diagnostic and prognostic markers for breast cancer. For example, magnetic resonance elastography has proven effective in identifying malignant tumors by detecting alterations in stiffness within the breast tissue [74, 240]. Integrating

techniques used to assess the biophysical characteristics of the tumor microenvironment with image-based tools (mammography, MRI and ultrasound), and machine learning algorithms could further accelerate the development of advanced prognostic and diagnostic tools for breast cancer. Furthermore, recent advancements in microfluidics have led to the development of an assay that screens potential antimetastatic drugs and predicts the metastatic propensity of isolated breast cancer cells [239]. This technique has the potential to complement existing diagnostic assays and determine whether a patient is at an increased risk of metastasis [239]. In conclusion, a comprehensive understanding of the implications of the physical traits of breast cancer holds significant promise for driving advancements in diagnosis, prognosis, treatment selection, and ultimately improving patient outcomes.

**Acknowledgements** We extend our gratitude to Farnaz Hemmati and Farshad Amiri from Auburn University for their diligent efforts in meticulously reviewing the schematics. All figures were created with biorender.com.

**Author contributions** A.A. and P.M. wrote the manuscript and prepared Figs. 1 and 2; Tables 1, 2, 3, 4 and 5. T. A., L.A.A. and R.D.A. edited the manuscript and provided feedback. P.M. and R.D.A secured funding. P.M. supervised the study. All authors reviewed the manuscript.

**Funding** This work was supported, in part, by grants from the National Institute of General Medical Sciences (R35GM147101) to P.M., and the Breast Cancer Research Foundation of Alabama to P.M. and R.D.A.

**Data availability** Not applicable.

## Declarations

**Ethics approval and consent to participate** Not applicable.

**Informed consent** Not applicable.

**Competing interests** The authors declare no competing interests.

**Open Access** This article is licensed under a Creative Commons Attribution 4.0 International License, which permits use, sharing, adaptation, distribution and reproduction in any medium or format, as long as you give appropriate credit to the original author(s) and the source, provide a link to the Creative Commons licence, and indicate if changes were made. The images or other third party material in this article are included in the article's Creative Commons licence, unless indicated otherwise in a credit line to the material. If material is not included in the article's Creative Commons licence and your intended use is not permitted by statutory regulation or exceeds the permitted use, you will need to obtain permission directly from the copyright holder. To view a copy of this licence, visit <http://creativecommons.org/licenses/by/4.0/>.

## References

- Corben, A. D. (2013). Pathology of invasive breast disease. *Surgical Clinics of North America*, 93(2), 363–392. <https://doi.org/10.1016/j.suc.2013.01.003>.
- Arpino, G., Bardou, V. J., Clark, G. M., & Elledge, R. M. (2004). Infiltrating lobular carcinoma of the breast: Tumor characteristics and clinical outcome. *Breast Cancer Research*, 6(3), R149–156. <https://doi.org/10.1186/bcr767>.
- Perou, C. M., Sorlie, T., Eisen, M. B., van de Rijn, M., Jeffrey, S. S., Rees, C. A., et al. (2000). Molecular portraits of human breast tumours. *Nature*, 406(6797), 747–752. <https://doi.org/10.1038/35021093>.
- Johnson, K. S., Conant, E. F., & Soo, M. S. (2020). Molecular subtypes of breast cancer: A review for breast radiologists. *Journal of Breast Imaging*, 3(1), 12–24. <https://doi.org/10.1093/jbi/wbaa110>.
- Orrantia-Borunda, E., Anchondo-Nunez, P., Acuna-Aguilar, L. E., Gomez-Valles, F. O., & Ramirez-Valdespino, C. A. (2022). Subtypes of Breast Cancer. In H. N. Mayrovitz (Ed.), *Breast Cancer*. Brisbane (AU).
- Siegel, R. L., Miller, K. D., Fuchs, H. E., & Jemal, A. (2022). Cancer statistics, 2022. *C Ca: A Cancer Journal for Clinicians*, 72(1), 7–33. <https://doi.org/10.3322/caac.21708>.
- Paul, C. D., Mistriotis, P., & Konstantopoulos, K. (2017). Cancer cell motility: Lessons from migration in confined spaces. *Nature Reviews Cancer*, 17(2), 131–140. <https://doi.org/10.1038/nrc.2016.123>.
- Wirtz, D., Konstantopoulos, K., & Searson, P. C. (2011). The physics of cancer: The role of physical interactions and mechanical forces in metastasis. *Nature Reviews Cancer*, 11(7), 512–522. <https://doi.org/10.1038/nrc3080>.
- Nia, H. T., Munn, L. L., & Jain, R. K. (2020). Physical traits of cancer. *Science*, 370(6516). <https://doi.org/10.1126/science.aaz0868>.
- Bera, K., Kiepas, A., Zhang, Y., Sun, S. X., & Konstantopoulos, K. (2022). The interplay between physical cues and mechanosensitive ion channels in cancer metastasis. *Front Cell Dev Biol*, 10, 954099. <https://doi.org/10.3389/fcell.2022.954099>.
- Heldin, C. H., Rubin, K., Pietras, K., & Ostman, A. (2004). High interstitial fluid pressure - an obstacle in cancer therapy. *Nature Reviews Cancer*, 4(10), 806–813. <https://doi.org/10.1038/nrc1456>.
- Nathanson, S. D., & Nelson, L. (1994). Interstitial fluid pressure in breast cancer, benign breast conditions, and breast parenchyma. *Annals of Surgical Oncology*, 1(4), 333–338. <https://doi.org/10.1007/BF03187139>.
- Hashizume, H., Baluk, P., Morikawa, S., McLean, J. W., Thurston, G., Roberge, S., et al. (2000). Openings between defective endothelial cells explain tumor vessel leakiness. *American Journal of Pathology*, 156(4), 1363–1380. [https://doi.org/10.1016/S0002-9440\(10\)65006-7](https://doi.org/10.1016/S0002-9440(10)65006-7).
- Jain, R. K. (2001). Delivery of molecular medicine to solid tumors: Lessons from in vivo imaging of gene expression and function. *Journal of Controlled Release : Official Journal of the Controlled Release Society*, 74(1–3), 7–25. [https://doi.org/10.1016/s0168-3659\(01\)00306-6](https://doi.org/10.1016/s0168-3659(01)00306-6).
- Greenberg, J. I., & Cheresh, D. A. (2009). VEGF as an inhibitor of tumor vessel maturation: Implications for cancer therapy. *Expert Opinion on Biological Therapy*, 9(11), 1347–1356. <https://doi.org/10.1517/14712590903208883>.
- De Bock, K., Cauwenberghs, S., & Carmeliet, P. (2011). Vessel abnormalization: Another hallmark of cancer? Molecular mechanisms and therapeutic implications. *Current Opinion in Genetics & Development*, 21(1), 73–79. <https://doi.org/10.1016/j.gde.2010.10.008>.
- Leu, A. J., Berk, D. A., Lymboussaki, A., Alitalo, K., & Jain, R. K. (2000). Absence of functional lymphatics within a murine sarcoma: A molecular and functional evaluation. *Cancer Research*, 60(16), 4324–4327.
- Wu, M., Frieboes, H. B., McDougall, S. R., Chaplain, M. A., Cristini, V., & Lowengrub, J. (2013). The effect of interstitial pressure on tumor growth: Coupling with the blood and lymphatic vascular systems. *Journal of Theoretical Biology*, 320, 131–151. <https://doi.org/10.1016/j.jtbi.2012.11.031>.
- Less, J. R., Posner, M. C., Boucher, Y., Borochovitz, D., Wolmark, N., & Jain, R. K. (1992). Interstitial hypertension in human breast and colorectal tumors. *Cancer Research*, 52(22), 6371–6374.
- Dadiani, M., Kalchenko, V., Yosepovich, A., Margalit, R., Hassid, Y., Degani, H., et al. (2006). Real-time imaging of lymphogenic metastasis in orthotopic human breast cancer. *Cancer Research*, 66(16), 8037–8041. <https://doi.org/10.1158/0008-5472.CAN-06-0728>.
- Ferretti, S., Allegrini, P. R., Becquet, M. M., & McSheehy, P. M. (2009). Tumor interstitial fluid pressure as an early-response marker for anticancer therapeutics. *Neoplasia (New York, N.Y.)*, 11(9), 874–881. <https://doi.org/10.1593/neo.09554>.
- Kim, S., Decarlo, L., Cho, G. Y., Jensen, J. H., Sodickson, D. K., Moy, L., et al. (2012). Interstitial fluid pressure correlates with intravoxel incoherent motion imaging metrics in a mouse mammary carcinoma model. *Nmr in Biomedicine*, 25(5), 787–794. <https://doi.org/10.1002/nbm.1793>.
- Islam, M. T., Tang, S., Tasciotti, E., & Righetti, R. (2021). Non-invasive Assessment of the spatial and temporal distributions of interstitial fluid pressure, Fluid Velocity and Fluid Flow in Cancers in vivo. *Ieee Access : Practical Innovations. Open Solutions*, 9, 89222–89233. <https://doi.org/10.1109/ACCESS.2021.3089454>.
- Hassid, Y., Furman-Haran, E., Margalit, R., Eilam, R., & Degani, H. (2006). Noninvasive magnetic resonance imaging of transport and interstitial fluid pressure in ectopic human lung tumors. *Cancer Research*, 66(8), 4159–4166. <https://doi.org/10.1158/0008-5472.CAN-05-3289>.
- Boucher, Y., Baxter, L. T., & Jain, R. K. (1990). Interstitial pressure gradients in tissue-isolated and subcutaneous tumors: Implications for therapy. *Cancer Research*, 50(15), 4478–4484.
- Jain, R. K., & Baxter, L. T. (1988). Mechanisms of heterogeneous distribution of monoclonal antibodies and other macromolecules in tumors: Significance of elevated interstitial pressure. *Cancer Research*, 48(24 Pt 1), 7022–7032.
- Chauhan, V. P., Stylianopoulos, T., Boucher, Y., & Jain, R. K. (2011). Delivery of molecular and nanoscale medicine to tumors: Transport barriers and strategies. *Annu Rev Chem Biomol Eng*, 2, 281–298. <https://doi.org/10.1146/annurev-chembioeng-061010-114300>.
- Stylianopoulos, T., & Jain, R. K. (2013). Combining two strategies to improve perfusion and drug delivery in solid tumors. *Proc Natl Acad Sci U S A*, 110(46), 18632–18637. <https://doi.org/10.1073/pnas.1318415110>.
- Tong, R. T., Boucher, Y., Kozin, S. V., Winkler, F., Hicklin, D. J., & Jain, R. K. (2004). Vascular normalization by vascular endothelial growth factor receptor 2 blockade induces a pressure gradient across the vasculature and improves drug penetration in tumors. *Cancer Research*, 64(11), 3731–3736. <https://doi.org/10.1158/0008-5472.CAN-04-0074>.
- Chauhan, V. P., Stylianopoulos, T., Martin, J. D., Popovic, Z., Chen, O., Kamoun, W. S., et al. (2012). Normalization of tumour blood vessels improves the delivery of nanomedicines in a size-dependent manner. *Nature Nanotechnology*, 7(6), 383–388. <https://doi.org/10.1038/nnano.2012.45>.

31. Meng, L., Gan, S., Zhou, Y., Cheng, Y., Ding, Y., Tong, X., et al. (2018). Oxygen-rich chemotherapy via modified Abraxane to inhibit the growth and metastasis of triple-negative breast cancer. *Biomater Sci*, 7(1), 168–177. <https://doi.org/10.1039/c8bm00753e>.
32. Chen, Q., Liang, C., Wang, C., & Liu, Z. (2015). An imagable and photothermal abraxane-like nanodrug for combination cancer therapy to treat subcutaneous and metastatic breast tumors. *Advanced Materials*, 27(5), 903–910. <https://doi.org/10.1002/adma.201404308>.
33. Fukumura, D., Kloepper, J., Amoozgar, Z., Duda, D. G., & Jain, R. K. (2018). Enhancing cancer immunotherapy using antiangiogenics: Opportunities and challenges. *Nature Reviews Clinical Oncology*, 15(5), 325–340. <https://doi.org/10.1038/nrclinonc.2018.29>.
34. Kazazi-Hyseni, F., Beijnen, J. H., & Schellens, J. H. (2010). *Bevacizumab Oncologist*, 15(8), 819–825, doi:<https://doi.org/10.1634/theoncologist.2009-0317>.
35. Miller, K., Wang, M., Gralow, J., Dickler, M., Cobleigh, M., Perez, E. A., et al. (2007). Paclitaxel plus Bevacizumab versus paclitaxel alone for metastatic breast cancer. *New England Journal of Medicine*, 357(26), 2666–2676. <https://doi.org/10.1056/NEJMoa072113>.
36. Brufsky, A. M., Hurvitz, S., Perez, E., Swamy, R., Valero, V., O'Neill, V., et al. (2011). RIBBON-2: A randomized, double-blind, placebo-controlled, phase III trial evaluating the efficacy and safety of bevacizumab in combination with chemotherapy for second-line treatment of human epidermal growth factor receptor 2-negative metastatic breast cancer. *Journal of Clinical Oncology*, 29(32), 4286–4293. <https://doi.org/10.1200/JCO.2010.34.1255>.
37. Robert, N. J., Dieras, V., Glaspy, J., Brufsky, A. M., Bondarenko, I., Lipatov, O. N., et al. (2011). RIBBON-1: Randomized, double-blind, placebo-controlled, phase III trial of chemotherapy with or without bevacizumab for first-line treatment of human epidermal growth factor receptor 2-negative, locally recurrent or metastatic breast cancer. *Journal of Clinical Oncology*, 29(10), 1252–1260. <https://doi.org/10.1200/JCO.2010.28.0982>.
38. Gianni, L., Romieu, G. H., Lichinitser, M., Serrano, S. V., Mansutti, M., Pivot, X., et al. (2013). AVEREL: A randomized phase III trial evaluating bevacizumab in combination with docetaxel and trastuzumab as first-line therapy for HER2-positive locally recurrent/metastatic breast cancer. *Journal of Clinical Oncology*, 31(14), 1719–1725. <https://doi.org/10.1200/JCO.2012.44.7912>.
39. Jain, R. K. (2014). Antiangiogenesis strategies revisited: From starving tumors to alleviating hypoxia. *Cancer Cell*, 26(5), 605–622. <https://doi.org/10.1016/j.ccr.2014.10.006>.
40. Ramjiawan, R. R., Griffioen, A. W., & Duda, D. G. (2017). Antiangiogenesis for cancer revisited: Is there a role for combinations with immunotherapy? *Angiogenesis*, 20(2), 185–204. <https://doi.org/10.1007/s10456-017-9552-y>.
41. Belotti, D., Vergani, V., Drudis, T., Borsotti, P., Pitelli, M. R., Viale, G., et al. (1996). The microtubule-affecting drug paclitaxel has antiangiogenic activity. *Clinical Cancer Research*, 2(11), 1843–1849.
42. Vacca, A., Ribatti, D., Iurlaro, M., Merchionne, F., Nico, B., Ria, R., et al. (2002). Docetaxel versus paclitaxel for antiangiogenesis. *J Hematother Stem Cell Res*, 11(1), 103–118. <https://doi.org/10.1089/152581602753448577>.
43. Hotchkiss, K. A., Ashton, A. W., Mahmood, R., Russell, R. G., Sparano, J. A., & Schwartz, E. L. (2002). Inhibition of endothelial cell function in vitro and angiogenesis in vivo by docetaxel (Taxotere): Association with impaired repositioning of the microtubule organizing center. *Molecular Cancer Therapeutics*, 1(13), 1191–1200.
44. Grant, D. S., Williams, T. L., Zahaczewsky, M., & Dicker, A. P. (2003). Comparison of antiangiogenic activities using paclitaxel (taxol) and docetaxel (taxotere). *International Journal of Cancer*, 104(1), 121–129. <https://doi.org/10.1002/ijc.10907>.
45. Griffon-Etienne, G., Boucher, Y., Brekken, C., Suit, H. D., & Jain, R. K. (1999). Taxane-induced apoptosis decompresses blood vessels and lowers interstitial fluid pressure in solid tumors: Clinical implications. *Cancer Research*, 59(15), 3776–3782.
46. Taghian, A. G., Abi-Raad, R., Assaad, S. I., Casty, A., Ancukiewicz, M., Yeh, E., et al. (2005). Paclitaxel decreases the interstitial fluid pressure and improves oxygenation in breast cancers in patients treated with neoadjuvant chemotherapy: Clinical implications. *Journal of Clinical Oncology*, 23(9), 1951–1961. <https://doi.org/10.1200/JCO.2005.08.119>.
47. Gao, M., Berghaus, M., Mobitz, S., Schuabb, V., Erwin, N., Herzog, M., et al. (2018). On the origin of microtubules' high-pressure sensitivity. *Biophys J*, 114(5), 1080–1090. <https://doi.org/10.1016/j.bpj.2018.01.021>.
48. Nishiyama, M. (2017). High-pressure microscopy for tracking dynamic properties of molecular machines. *Biophysical Chemistry*, 231, 71–78. <https://doi.org/10.1016/j.bpc.2017.03.010>.
49. Nishiyama, M., Kimura, Y., Nishiyama, Y., & Terazima, M. (2009). Pressure-induced changes in the structure and function of the kinesin-microtubule complex. *Biophys J*, 96(3), 1142–1150. <https://doi.org/10.1016/j.bpj.2008.10.023>.
50. Zhao, R., Afthinos, A., Zhu, T., Mistriotis, P., Li, Y., Serra, S. A., et al. (2019). Cell sensing and decision-making in confinement: The role of TRPM7 in a tug of war between hydraulic pressure and cross-sectional area. *Science Advances*, 5(7), eaaw7243. <https://doi.org/10.1126/sciadv.aaw7243>.
51. Diresta, G. R., Nathan, S. S., Manoso, M. W., Casas-Ganem, J., Wyatt, C., Kubo, T., et al. (2005). Cell proliferation of cultured human cancer cells are affected by the elevated tumor pressures that exist in vivo. *Annals of Biomedical Engineering*, 33(9), 1270–1280. <https://doi.org/10.1007/s10439-005-5732-9>.
52. Kao, Y. C., Jheng, J. R., Pan, H. J., Liao, W. Y., Lee, C. H., & Kuo, P. L. (2017). Elevated hydrostatic pressure enhances the motility and enlarges the size of the lung cancer cells through aquaporin upregulation mediated by caveolin-1 and ERK1/2 signaling. *Oncogene*, 36(6), 863–874. <https://doi.org/10.1038/onc.2016.255>.
53. Shang, M., Lim, S. B., Jiang, K., Yap, Y. S., Khoo, B. L., Han, J., et al. (2021). Microfluidic studies of hydrostatic pressure-enhanced doxorubicin resistance in human breast cancer cells. *Lab on a Chip*, 21(4), 746–754. <https://doi.org/10.1039/d0lc01103g>.
54. Friman, T., Gustafsson, R., Stuhr, L. B., Chidac, J., Heldin, N. E., Reed, R. K., et al. (2012). Increased fibrosis and interstitial fluid pressure in two different types of syngeneic murine carcinoma grown in integrin beta3-subunit deficient mice. *PLoS One*, 7(3), e34082. <https://doi.org/10.1371/journal.pone.0034082>.
55. Smeland, H. Y., Lu, N., Karlsen, T. V., Salvesen, G., Reed, R. K., & Stuhr, L. (2019). Stromal integrin alpha11-deficiency reduces interstitial fluid pressure and perturbs collagen structure in triple-negative breast xenograft tumors. *Bmc Cancer*, 19(1), 234. <https://doi.org/10.1186/s12885-019-5449-z>.
56. Insua-Rodriguez, J., & Oskarsson, T. (2016). The extracellular matrix in breast cancer. *Advanced Drug Delivery Reviews*, 97, 41–55. <https://doi.org/10.1016/j.addr.2015.12.017>.
57. Ronnov-Jessen, L., Petersen, O. W., Kotelansky, V. E., & Bissell, M. J. (1995). The origin of the myofibroblasts in breast cancer. Recapitulation of tumor environment in culture unravels diversity and implicates converted fibroblasts and recruited smooth muscle cells. *J Clin Invest*, 95(2), 859–873. <https://doi.org/10.1172/JCI117736>.
58. Bochet, L., Lehuede, C., Dauvillier, S., Wang, Y. Y., Dirat, B., Laurent, V., et al. (2013). Adipocyte-derived fibroblasts promote tumor progression and contribute to the desmoplastic reaction in

- breast cancer. *Cancer Research*, 73(18), 5657–5668. <https://doi.org/10.1158/0008-5472.CAN-13-0530>.
59. Raz, Y., Cohen, N., Shani, O., Bell, R. E., Novitskiy, S. V., Abramovitz, L., et al. (2018). Bone marrow-derived fibroblasts are a functionally distinct stromal cell population in breast cancer. *Journal of Experimental Medicine*, 215(12), 3075–3093. <https://doi.org/10.1084/jem.20180818>.
  60. Avgustinova, A., Iravani, M., Robertson, D., Fearns, A., Gao, Q., Klingbeil, P., et al. (2016). Tumour cell-derived Wnt7a recruits and activates fibroblasts to promote tumour aggressiveness. *Nature Communications*, 7, 10305. <https://doi.org/10.1038/ncomms10305>.
  61. Sharon, Y., Raz, Y., Cohen, N., Ben-Shmuel, A., Schwartz, H., Geiger, T., et al. (2015). Tumor-derived osteopontin reprograms normal mammary fibroblasts to promote inflammation and tumor growth in breast cancer. *Cancer Research*, 75(6), 963–973. <https://doi.org/10.1158/0008-5472.CAN-14-1990>.
  62. Butti, R., Nimma, R., Kundu, G., Bulbuli, A., Kumar, T. V. S., Gunasekaran, V. P., et al. (2021). Tumor-derived osteopontin drives the resident fibroblast to myofibroblast differentiation through Twist1 to promote breast cancer progression. *Oncogene*, 40(11), 2002–2017. <https://doi.org/10.1038/s41388-021-01663-2>.
  63. Baroni, S., Romero-Cordoba, S., Plantamura, I., Dugo, M., D'Ippolito, E., Cataldo, A., et al. (2016). Exosome-mediated delivery of miR-9 induces cancer-associated fibroblast-like properties in human breast fibroblasts. *Cell Death and Disease*, 7(7), e2312. <https://doi.org/10.1038/cddis.2016.224>.
  64. Vu, L. T., Peng, B., Zhang, D. X., Ma, V., Mathey-Andrews, C. A., Lam, C. K., et al. (2019). Tumor-secreted extracellular vesicles promote the activation of cancer-associated fibroblasts via the transfer of microRNA-125b. *J Extracell Vesicles*, 8(1), 1599680. <https://doi.org/10.1080/20013078.2019.1599680>.
  65. Li, K., Liu, T., Chen, J., Ni, H., & Li, W. (2020). Survivin in breast cancer-derived exosomes activates fibroblasts by up-regulating SOD1, whose feedback promotes cancer proliferation and metastasis. *Journal of Biological Chemistry*, 295(40), 13737–13752. <https://doi.org/10.1074/jbc.RA120.013805>.
  66. Hu, D., Li, Z., Zheng, B., Lin, X., Pan, Y., Gong, P., et al. (2022). Cancer-associated fibroblasts in breast cancer: Challenges and opportunities. *Cancer Commun (Lond)*, 42(5), 401–434. <https://doi.org/10.1002/cac2.12291>.
  67. Zellmer, V. R., Schnepf, P. M., Fracci, S. L., Tan, X., Howe, E. N., & Zhang, S. (2017). Tumor-induced stromal STAT1 accelerates breast Cancer via deregulating tissue homeostasis. *Molecular Cancer Research*, 15(5), 585–597. <https://doi.org/10.1158/1541-7786.MCR-16-0312>.
  68. Erez, N., Truitt, M., Olson, P., Arron, S. T., & Hanahan, D. (2010). Cancer-Associated fibroblasts are activated in Incipient Neoplasia to Orchestrate Tumor-promoting inflammation in an NF-kappaB-dependent manner. *Cancer Cell*, 17(2), 135–147. <https://doi.org/10.1016/j.ccr.2009.12.041>.
  69. Casey, T., Bond, J., Tighe, S., Hunter, T., Lintault, L., Patel, O., et al. (2009). Molecular signatures suggest a major role for stromal cells in development of invasive breast cancer. *Breast Cancer Research and Treatment*, 114(1), 47–62. <https://doi.org/10.1007/s10549-008-9982-8>.
  70. Levental, K. R., Yu, H., Kass, L., Lakins, J. N., Egeblad, M., Erler, J. T., et al. (2009). Matrix crosslinking forces tumor progression by enhancing integrin signaling. *Cell*, 139(5), 891–906. <https://doi.org/10.1016/j.cell.2009.10.027>.
  71. Han, Y. L., Ronceray, P., Xu, G., Malandrino, A., Kamm, R. D., Lenz, M., et al. (2018). Cell contraction induces long-ranged stress stiffening in the extracellular matrix. *Proc Natl Acad Sci U S A*, 115(16), 4075–4080. <https://doi.org/10.1073/pnas.1722619115>.
  72. Hayashi, M., Yamamoto, Y., Ibusuki, M., Fujiwara, S., Yamamoto, S., Tomita, S., et al. (2012). Evaluation of tumor stiffness by elastography is predictive for pathologic complete response to neoadjuvant chemotherapy in patients with breast cancer. *Annals of Surgical Oncology*, 19(9), 3042–3049. <https://doi.org/10.1245/s10434-012-2343-1>.
  73. Boyd, N. F., Li, Q., Melnichouk, O., Huszti, E., Martin, L. J., Gunasekara, A., et al. (2014). Evidence that breast tissue stiffness is associated with risk of breast cancer. *PLoS One*, 9(7), e100937. <https://doi.org/10.1371/journal.pone.0100937>.
  74. Barba, D., Leon-Sosa, A., Lugo, P., Suquillo, D., Torres, F., Surre, F., et al. (2021). Breast cancer, screening and diagnostic tools: All you need to know. *Critical Reviews in Oncology Hematology*, 157, 103174. <https://doi.org/10.1016/j.critrevonc.2020.103174>.
  75. Acerbi, I., Cassereau, L., Dean, I., Shi, Q., Au, A., Park, C., et al. (2015). Human breast cancer invasion and aggression correlates with ECM stiffening and immune cell infiltration. *Integr Biol (Camb)*, 7(10), 1120–1134. <https://doi.org/10.1039/c5ib00040h>.
  76. Bordeleau, F., Mason, B. N., Lollis, E. M., Mazzola, M., Zanotelli, M. R., Somasegar, S., et al. (2017). Matrix stiffening promotes a tumor vasculature phenotype. *Proc Natl Acad Sci U S A*, 114(3), 492–497. <https://doi.org/10.1073/pnas.1613855114>.
  77. Paszek, M. J., Zahir, N., Johnson, K. R., Lakins, J. N., Rosenberg, G. I., Gefen, A., et al. (2005). Tensional homeostasis and the malignant phenotype. *Cancer Cell*, 8(3), 241–254. <https://doi.org/10.1016/j.ccr.2005.08.010>.
  78. Pang, M. F., Siedlik, M. J., Han, S., Stallings-Mann, M., Radisky, D. C., & Nelson, C. M. (2016). Tissue stiffness and Hypoxia modulate the integrin-linked kinase ILK to control breast Cancer stem-like cells. *Cancer Research*, 76(18), 5277–5287. <https://doi.org/10.1158/0008-5472.CAN-16-0579>.
  79. Wei, S. C., Fattet, L., Tsai, J. H., Guo, Y., Pai, V. H., Majeski, H. E., et al. (2015). Matrix stiffness drives epithelial-mesenchymal transition and tumour metastasis through a TWIST1-G3BP2 mechanotransduction pathway. *Nature Cell Biology*, 17(5), 678–688. <https://doi.org/10.1038/ncb3157>.
  80. Jolly, M. K., Boareto, M., Huang, B., Jia, D., Lu, M., Ben-Jacob, E., et al. (2015). Implications of the hybrid Epithelial/Mesenchymal phenotype in Metastasis. *Frontiers in Oncology*, 5, 155. <https://doi.org/10.3389/fonc.2015.00155>.
  81. Neelakantan, D., Zhou, H., Oliphant, M. U. J., Zhang, X., Simon, L. M., Henke, D. M., et al. (2017). EMT cells increase breast cancer metastasis via paracrine GLI activation in neighbouring tumour cells. *Nature Communications*, 8, 15773. <https://doi.org/10.1038/ncomms15773>.
  82. Lo, C. M., Wang, H. B., Dembo, M., & Wang, Y. L. (2000). Cell movement is guided by the rigidity of the substrate. *Biophys J*, 79(1), 144–152. [https://doi.org/10.1016/S0006-3495\(00\)76279-5](https://doi.org/10.1016/S0006-3495(00)76279-5).
  83. Pelham, R. J. Jr., & Wang, Y. (1997). Cell locomotion and focal adhesions are regulated by substrate flexibility. *Proc Natl Acad Sci U S A*, 94(25), 13661–13665. <https://doi.org/10.1073/pnas.94.25.13661>.
  84. Hamidi, H., & Ivaska, J. (2018). Every step of the way: Integrins in cancer progression and metastasis. *Nature Reviews Cancer*, 18(9), 533–548. <https://doi.org/10.1038/s41568-018-0038-z>.
  85. Dupont, S., Morsut, L., Aragona, M., Enzo, E., Giulitti, S., Cordeonsi, M., et al. (2011). Role of YAP/TAZ in mechanotransduction. *Nature*, 474(7350), 179–183. <https://doi.org/10.1038/nature10137>.
  86. Meng, Z., Qiu, Y., Lin, K. C., Kumar, A., Placone, J. K., Fang, C., et al. (2018). RAP2 mediates mechanoresponses of the Hippo pathway. *Nature*, 560(7720), 655–660. <https://doi.org/10.1038/s41586-018-0444-0>.
  87. Calvo, F., Ege, N., Grande-Garcia, A., Hooper, S., Jenkins, R. P., Chaudhry, S. I., et al. (2013). Mechanotransduction and YAP-dependent matrix remodelling is required for the generation and maintenance of cancer-associated fibroblasts. *Nature Cell Biology*, 15(6), 637–646. <https://doi.org/10.1038/ncb2756>.

88. Yuan, M., Tomlinson, V., Lara, R., Holliday, D., Chelala, C., Harada, T., et al. (2008). Yes-associated protein (YAP) functions as a tumor suppressor in breast. *Cell Death and Differentiation*, 15(11), 1752–1759. <https://doi.org/10.1038/cdd.2008.108>.
89. Lee, J. Y., Chang, J. K., Dominguez, A. A., Lee, H. P., Nam, S., Chang, J., et al. (2019). YAP-independent mechanotransduction drives breast cancer progression. *Nature Communications*, 10(1), 1848. <https://doi.org/10.1038/s41467-019-09755-0>.
90. Afthinos, A., Bera, K., Chen, J., Ozcelikkale, A., Amitrano, A., Choudhury, M. I., et al. (2022). Migration and 3D Traction Force measurements inside compliant microchannels. *Nano Letters*, 22(18), 7318–7327. <https://doi.org/10.1021/acs.nanolett.2c01261>.
91. Chan, C. E., & Odde, D. J. (2008). Traction dynamics of filopodia on compliant substrates. *Science*, 322(5908), 1687–1691. <https://doi.org/10.1126/science.1163595>.
92. Bangasser, B. L., Rosenfeld, S. S., & Odde, D. J. (2013). Determinants of maximal force transmission in a motor-clutch model of cell traction in a compliant microenvironment. *Biophys J*, 105(3), 581–592. <https://doi.org/10.1016/j.bpj.2013.06.027>.
93. Bangasser, B. L., Shamsan, G. A., Chan, C. E., Opoku, K. N., Tuzel, E., Schlichtmann, B. W., et al. (2017). Shifting the optimal stiffness for cell migration. *Nature Communications*, 8, 15313. <https://doi.org/10.1038/ncomms15313>.
94. Elosegui-Artola, A., Orias, R., Chen, Y., Kosmalska, A., Perez-Gonzalez, C., Castro, N., et al. (2016). Mechanical regulation of a molecular clutch defines force transmission and transduction in response to matrix rigidity. *Nature Cell Biology*, 18(5), 540–548. <https://doi.org/10.1038/ncb3336>.
95. DuChez, B. J., Doyle, A. D., Dimitriadis, E. K., & Yamada, K. M. (2019). Durotaxis by Human Cancer cells. *Biophys J*, 116(4), 670–683. <https://doi.org/10.1016/j.bpj.2019.01.009>.
96. Isomursu, A., Park, K. Y., Hou, J., Cheng, B., Mathieu, M., Shamsan, G. A., et al. (2022). Directed cell migration towards softer environments. *Nature Materials*, 21(9), 1081–1090. <https://doi.org/10.1038/s41563-022-01294-2>.
97. Kagan, H. M., & Li, W. (2003). Lysyl oxidase: Properties, specificity, and biological roles inside and outside of the cell. *Journal of Cellular Biochemistry*, 88(4), 660–672. <https://doi.org/10.1002/jcb.10413>.
98. Schmelzer, C. E. H., Heinz, A., Troilo, H., Lockhart-Cairns, M. P., Jowitt, T. A., Marchand, M. F., et al. (2019). Lysyl oxidase-like 2 (LOXL2)-mediated cross-linking of tropoelastin. *The Faseb Journal*, 33(4), 5468–5481. <https://doi.org/10.1096/fj.201801860RR>.
99. Saatci, O., Kaymak, A., Raza, U., Ersan, P. G., Akbulut, O., Bannister, C. E., et al. (2020). Targeting lysyl oxidase (LOX) overcomes chemotherapy resistance in triple negative breast cancer. *Nature Communications*, 11(1), 2416. <https://doi.org/10.1038/s41467-020-16199-4>.
100. Zhu, S., Zhang, T., Gao, H., Jin, G., Yang, J., He, X., et al. (2023). Combination therapy of lox inhibitor and stimuli-responsive drug for Mechanocchemically synergistic breast Cancer Treatment. *Adv Healthc Mater*, 12(21), e2300103. <https://doi.org/10.1002/adhm.202300103>.
101. Barker, H. E., Chang, J., Cox, T. R., Lang, G., Bird, D., Nicolau, M., et al. (2011). LOXL2-mediated matrix remodeling in metastasis and mammary gland involution. *Cancer Research*, 71(5), 1561–1572. <https://doi.org/10.1158/0008-5472.CAN-10-2868>.
102. Benson, A. B. 3rd, Wainberg, Z. A., Hecht, J. R., Vyushkov, D., Dong, H., Bendell, J., et al. (2017). A phase II randomized, Double-Blind, placebo-controlled study of Simtuzumab or Placebo in Combination with Gemcitabine for the First-Line treatment of pancreatic adenocarcinoma. *The Oncologist*, 22(3), 241–e215. <https://doi.org/10.1634/theoncologist.2017-0024>.
103. Hecht, J. R., Benson, A. B. 3rd, Vyushkov, D., Yang, Y., Bendell, J., & Verma, U. (2017). A phase II, Randomized, Double-Blind, placebo-controlled study of Simtuzumab in Combination with FOLFIRI for the second-line treatment of metastatic KRAS Mutant Colorectal Adenocarcinoma. *The Oncologist*, 22(3), 243–e223. <https://doi.org/10.1634/theoncologist.2016-0479>.
104. Golatta, M., Schweitzer-Martin, M., Harcos, A., Schott, S., Junkermann, H., Rauch, G., et al. (2013). Normal breast tissue stiffness measured by a new ultrasound technique: Virtual touch tissue imaging quantification (VTIQ). *European Journal of Radiology*, 82(11), e676–679. <https://doi.org/10.1016/j.ejrad.2013.06.029>.
105. Youk, J. H., Son, E. J., Park, A. Y., & Kim, J. A. (2014). Shear-wave elastography for breast masses: Local shear wave speed (m/sec) versus young modulus (kPa). *Ultrasonography*, 33(1), 34–39. <https://doi.org/10.14366/usg.13005>.
106. Sinkus, R., Tanter, M., Xydeas, T., Catheline, S., Bercoff, J., & Fink, M. (2005). Viscoelastic shear properties of in vivo breast lesions measured by MR Elastography. *Magnetic Resonance Imaging*, 23(2), 159–165. <https://doi.org/10.1016/j.mri.2004.11.060>.
107. Xydeas, T., Siegmund, K., Sinkus, R., Krainick-Strobel, U., Miller, S., & Claussen, C. D. (2005). Magnetic resonance elastography of the breast: Correlation of signal intensity data with viscoelastic properties. *Investigative Radiology*, 40(7), 412–420. <https://doi.org/10.1097/01.rli.0000166940.72971.4a>.
108. Song, E. J., Sohn, Y. M., & Seo, M. (2018). Tumor stiffness measured by quantitative and qualitative shear wave elastography of breast cancer. *British Journal of Radiology*, 91(1086), 20170830. <https://doi.org/10.1259/bjr.20170830>.
109. Chang, J. M., Park, I. A., Lee, S. H., Kim, W. H., Bae, M. S., Koo, H. R., et al. (2013). Stiffness of tumours measured by shear-wave elastography correlated with subtypes of breast cancer. *European Radiology*, 23(9), 2450–2458. <https://doi.org/10.1007/s00330-013-2866-2>.
110. Yoo, J., Seo, B. K., Park, E. K., Kwon, M., Jeong, H., Cho, K. R., et al. (2020). Tumor stiffness measured by shear wave elastography correlates with tumor hypoxia as well as histologic biomarkers in breast cancer. *Cancer Imaging*, 20(1), 85. <https://doi.org/10.1186/s40644-020-00362-7>.
111. Nia, H. T., Liu, H., Seano, G., Datta, M., Jones, D., Rahbari, N., et al. (2016). Solid stress and elastic energy as measures of tumour mechanopathology. *Nat Biomed Eng*, 1, <https://doi.org/10.1038/s41551-016-0004>.
112. Padera, T. P., Stoll, B. R., Tooredman, J. B., Capen, D., di Tomaso, E., & Jain, R. K. (2004). Pathology: cancer cells compress intratumour vessels. *Nature*, 427(6976), 695. <https://doi.org/10.1038/427695a>.
113. Kalli, M., & Stylianopoulos, T. (2018). Defining the role of solid stress and Matrix Stiffness in Cancer Cell Proliferation and Metastasis. *Frontiers in Oncology*, 8, 55. <https://doi.org/10.3389/fonc.2018.00055>.
114. Jain, R. K., Martin, J. D., & Stylianopoulos, T. (2014). The role of mechanical forces in tumor growth and therapy. *Annual Review of Biomedical Engineering*, 16, 321–346. <https://doi.org/10.1146/annurev-bioeng-071813-105259>.
115. Stylianopoulos, T., Martin, J. D., Chauhan, V. P., Jain, S. R., Diop-Frimpong, B., Bardeesy, N., et al. (2012). Causes, consequences, and remedies for growth-induced solid stress in murine and human tumors. *Proc Natl Acad Sci U S A*, 109(38), 15101–15108. <https://doi.org/10.1073/pnas.1213353109>.
116. Zhang, S., Grifno, G., Passaro, R., Regan, K., Zheng, S., Hadzipasic, M., et al. (2023). Intravital measurements of solid stresses in tumours reveal length-scale and microenvironmentally dependent force transmission. *Nat Biomed Eng*, 7(11), 1473–1492. <https://doi.org/10.1038/s41551-023-01080-8>.

117. Helmlinger, G., Netti, P. A., Lichtenbeld, H. C., Melder, R. J., & Jain, R. K. (1997). Solid stress inhibits the growth of multicellular tumor spheroids. *Nature Biotechnology*, 15(8), 778–783. <https://doi.org/10.1038/nbt0897-778>.
118. Cheng, G., Tse, J., Jain, R. K., & Munn, L. L. (2009). Micro-environmental mechanical stress controls tumor spheroid size and morphology by suppressing proliferation and inducing apoptosis in cancer cells. *PLoS One*, 4(2), e4632. <https://doi.org/10.1371/journal.pone.0004632>.
119. Wong, S. H. D., Yin, B., Li, Z., Yuan, W., Zhang, Q., Xie, X., et al. (2023). Mechanical manipulation of cancer cell tumorigenicity via heat shock protein signaling. *Science Advances*, 9(27), eadg9593. <https://doi.org/10.1126/sciadv.adg9593>.
120. Tse, J. M., Cheng, G., Tyrrell, J. A., Wilcox-Adelman, S. A., Boucher, Y., Jain, R. K., et al. (2012). Mechanical compression drives cancer cells toward invasive phenotype. *Proc Natl Acad Sci U S A*, 109(3), 911–916. <https://doi.org/10.1073/pnas.1118910109>.
121. Luo, M., Cai, G., Ho, K. K. Y., Wen, K., Tong, Z., Deng, L., et al. (2022). Compression enhances invasive phenotype and matrix degradation of breast Cancer cells via Piezol activation. *BMC Mol Cell Biol*, 23(1), 1. <https://doi.org/10.1186/s12860-021-00401-6>.
122. Yeh, C. F., Juang, D. S., Chen, Y. W., Rodoplus, D., & Hsu, C. H. (2022). A portable controllable compressive stress device to monitor human breast Cancer cell protrusions at single-cell resolution. *Frontiers in Bioengineering and Biotechnology*, 10, 852318. <https://doi.org/10.3389/fbioe.2022.852318>.
123. Le Berre, M., Aubertin, J., & Piel, M. (2012). Fine control of nuclear confinement identifies a threshold deformation leading to lamina rupture and induction of specific genes. *Integr Biol (Camb)*, 4(11), 1406–1414. <https://doi.org/10.1039/c2ib20056b>.
124. Elosegui-Artola, A., Andreu, I., Beedle, A. E. M., Lezamiz, A., Uroz, M., Kosmalska, A. J., et al. (2017). Force triggers YAP Nuclear Entry by regulating transport across Nuclear pores. *Cell*, 171(6), 1397–1410e1314. <https://doi.org/10.1016/j.cell.2017.10.008>.
125. Andreu, I., Granero-Moya, I., Chahare, N. R., Clein, K., Molina-Jordan, M., Beedle, A. E. M., et al. (2022). Mechanical force application to the nucleus regulates nucleocytoplasmic transport. *Nature Cell Biology*, 24(6), 896–905. <https://doi.org/10.1038/s41556-022-00927-7>.
126. Kim, B. G., Gao, M. Q., Kang, S., Choi, Y. P., Lee, J. H., Kim, J. E., et al. (2017). Mechanical compression induces VEGFA overexpression in breast cancer via DNMT3A-dependent miR-9 downregulation. *Cell Death and Disease*, 8(3), e2646. <https://doi.org/10.1038/cddis.2017.73>.
127. Liu, J., Liao, S., Diop-Frimpong, B., Chen, W., Goel, S., Naxerova, K., et al. (2012). TGF-beta blockade improves the distribution and efficacy of therapeutics in breast carcinoma by normalizing the tumor stroma. *Proc Natl Acad Sci USA*, 109(41), 16618–16623. <https://doi.org/10.1073/pnas.1117610109>.
128. Chauhan, V. P., Martin, J. D., Liu, H., Lacorre, D. A., Jain, S. R., Kozin, S. V., et al. (2013). Angiotensin inhibition enhances drug delivery and potentiates chemotherapy by decompressing tumour blood vessels. *Nature Communications*, 4, 2516. <https://doi.org/10.1038/ncomms3516>.
129. Tang, Y., Liu, Y., Wang, S., Tian, Y., Li, Y., Teng, Z., et al. (2019). Depletion of collagen by losartan to improve tumor accumulation and therapeutic efficacy of photodynamic nanoplateforms. *Drug Deliv Transl Res*, 9(3), 615–624. <https://doi.org/10.1007/s13346-018-00610-1>.
130. Cun, X., Ruan, S., Chen, J., Zhang, L., Li, J., He, Q., et al. (2016). A dual strategy to improve the penetration and treatment of breast cancer by combining shrinking nanoparticles with collagen depletion by losartan. *Acta Biomaterialia*, 31, 186–196. <https://doi.org/10.1016/j.actbio.2015.12.002>.
131. Zhao, Q., He, X., Qin, X., Liu, Y., Jiang, H., Wang, J., et al. (2022). Enhanced therapeutic efficacy of combining Losartan and Chemo-Immunotherapy for Triple negative breast Cancer. *Frontiers in Immunology*, 13, 938439. <https://doi.org/10.3389/fimmu.2022.938439>.
132. Papageorgis, P., Polydorou, C., Mpekris, F., Voutouri, C., Agathokleous, E., Kapnissi-Christodoulou, C. P., et al. (2017). Tranilast-induced stress alleviation in solid tumors improves the efficacy of chemo- and nanotherapeutics in a size-independent manner. *Scientific Reports*, 7, 46140. <https://doi.org/10.1038/srep46140>.
133. Voutouri, C., & Stylianopoulos, T. (2018). Accumulation of mechanical forces in tumors is related to hyaluronan content and tissue stiffness. *PLoS One*, 13(3), e0193801. <https://doi.org/10.1371/journal.pone.0193801>.
134. Polydorou, C., Mpekris, F., Papageorgis, P., Voutouri, C., & Stylianopoulos, T. (2017). Pirfenidone normalizes the tumor microenvironment to improve chemotherapy. *Oncotarget*, 8(15), 24505–24517. <https://doi.org/10.1863/oncotarget.15534>.
135. Formenti, S. C., Lee, P., Adams, S., Goldberg, J. D., Li, X., Xie, M. W., et al. (2018). Focal irradiation and systemic TGFbeta blockade in metastatic breast Cancer. *Clinical Cancer Research*, 24(11), 2493–2504. <https://doi.org/10.1158/1078-0432.CCR-17-3322>.
136. Hingorani, S. R., Zheng, L., Bullock, A. J., Seery, T. E., Harris, W. P., Sigal, D. S., et al. (2018). HALO 202: Randomized Phase II study of PEGPH20 plus Nab-Paclitaxel/Gemcitabine versus Nab-Paclitaxel/Gemcitabine in patients with untreated, metastatic pancreatic ductal adenocarcinoma. *Journal of Clinical Oncology*, 36(4), 359–366. <https://doi.org/10.1200/JCO.2017.74.9564>.
137. Mierke, C. T. (2021). Viscoelasticity acts as a marker for Tumor Extracellular Matrix characteristics. *Front Cell Dev Biol*, 9, 785138. <https://doi.org/10.3389/fcell.2021.785138>.
138. Chaudhuri, O., Cooper-White, J., Janmey, P. A., Mooney, D. J., & Shenoy, V. B. (2020). Effects of extracellular matrix viscoelasticity on cellular behaviour. *Nature*, 584(7822), 535–546. <https://doi.org/10.1038/s41586-020-2612-2>.
139. Bayat, M., Nabavizadeh, A., Kumar, V., Gregory, A., Insana, M., Alizad, A., et al. (2018). Automated in vivo Sub-hertz Analysis of Viscoelasticity (SAVE) for evaluation of breast lesions. *Ieee Transactions on Biomedical Engineering*, 65(10), 2237–2247. <https://doi.org/10.1109/TBME.2017.2787679>.
140. Kumar, V., Denis, M., Gregory, A., Bayat, M., Mehrmohammadi, M., Fazzio, R., et al. (2018). Viscoelastic parameters as discriminators of breast masses: Initial human study results. *PLoS One*, 13(10), e0205717. <https://doi.org/10.1371/journal.pone.0205717>.
141. Sinkus, R., Siegmann, K., Xydeas, T., Tanter, M., Claussen, C., & Fink, M. (2007). MR elastography of breast lesions: Understanding the solid/liquid duality can improve the specificity of contrast-enhanced MR Mammography. *Magnetic Resonance in Medicine*, 58(6), 1135–1144. <https://doi.org/10.1002/mrm.21404>.
142. Nam, S., Gupta, V. K., Lee, H. P., Lee, J. Y., Wisdom, K. M., Varma, S., et al. (2019). Cell cycle progression in confining microenvironments is regulated by a growth-responsive TRPV4-PI3K/Akt-p27(Kip1) signaling axis. *Science Advances*, 5(8), eaaw6171. <https://doi.org/10.1126/sciadv.aaw6171>.
143. Adebawale, K., Gong, Z., Hou, J. C., Wisdom, K. M., Garbett, D., Lee, H. P., et al. (2021). Enhanced substrate stress relaxation promotes filopodia-mediated cell migration. *Nature Materials*, 20(9), 1290–1299. <https://doi.org/10.1038/s41563-021-00981-w>.
144. Wisdom, K. M., Adebawale, K., Chang, J., Lee, J. Y., Nam, S., Desai, R., et al. (2018). Matrix mechanical plasticity regulates cancer cell migration through confining microenvironments. *Nature Communications*, 9(1), 4144. <https://doi.org/10.1038/s41467-018-06641-z>.

145. Ban, E., Franklin, J. M., Nam, S., Smith, L. R., Wang, H., Wells, R. G., et al. (2018). Mechanisms of Plastic Deformation in Collagen Networks Induced by Cellular forces. *Biophys J*, 114(2), 450–461. <https://doi.org/10.1016/j.bpj.2017.11.3739>.
146. Weiss, L., Nannmark, U., Johansson, B. R., & Bagge, U. (1992). Lethal deformation of cancer cells in the microcirculation: A potential rate regulator of hematogenous metastasis. *International Journal of Cancer*, 50(1), 103–107. <https://doi.org/10.1002/ijc.2910500121>.
147. Weiss, L. (1992). Biomechanical interactions of cancer cells with the microvasculature during hematogenous metastasis. *Cancer and Metastasis Reviews*, 11(3–4), 227–235. <https://doi.org/10.1007/BF01307179>.
148. Wolf, K., Alexander, S., Schacht, V., Coussens, L. M., von Andrian, U. H., van Rheenen, J., et al. (2009). Collagen-based cell migration models in vitro and in vivo. *Seminars in Cell & Developmental Biology*, 20(8), 931–941. <https://doi.org/10.1016/j.semcdb.2009.08.005>.
149. Sahai, E., Wyckoff, J., Philippar, U., Segall, J. E., Gertler, F., & Condeelis, J. (2005). Simultaneous imaging of GFP, CFP and collagen in tumors in vivo using multiphoton microscopy. *Bmc Biotechnology*, 5, 14. <https://doi.org/10.1186/1472-6750-5-14>.
150. Weigelin, B., Bakker, G. J., & Friedl, P. (2012). Intravital third harmonic generation microscopy of collective melanoma cell invasion: Principles of interface guidance and microvesicle dynamics. *Intravital*, 1(1), 32–43. <https://doi.org/10.4161/intv.21223>.
151. Hung, W. C., Yang, J. R., Yankaskas, C. L., Wong, B. S., Wu, P. H., Pardo-Pastor, C., et al. (2016). Confinement sensing and Signal Optimization via Piez1/PKA and myosin II pathways. *Cell Rep*, 15(7), 1430–1441. <https://doi.org/10.1016/j.celrep.2016.04.035>.
152. Liu, Y. J., Le Berre, M., Lautenschlaeger, F., Maiuri, P., Callan-Jones, A., Heuze, M., et al. (2015). Confinement and low adhesion induce fast amoeboid migration of slow mesenchymal cells. *Cell*, 160(4), 659–672. <https://doi.org/10.1016/j.cell.2015.01.007>.
153. Balzer, E. M., Tong, Z., Paul, C. D., Hung, W. C., Stroka, K. M., Boggs, A. E., et al. (2012). Physical confinement alters tumor cell adhesion and migration phenotypes. *The Faseb Journal*, 26(10), 4045–4056. <https://doi.org/10.1096/fj.12-211441>.
154. Tong, Z., Balzer, E. M., Dallas, M. R., Hung, W. C., Stebe, K. J., & Konstantopoulos, K. (2012). Chemotaxis of cell populations through confined spaces at single-cell resolution. *PLoS One*, 7(1), e29211. <https://doi.org/10.1371/journal.pone.0029211>.
155. Wisniewski, E. O., Mistriotis, P., Bera, K., Law, R. A., Zhang, J., Nikolic, M., et al. (2020). Dorsoventral polarity directs cell responses to migration track geometries. *Science Advances*, 6(31), eaba6505. <https://doi.org/10.1126/sciadv.aba6505>.
156. Mitra Ghosh, T., Mazumder, S., Davis, J., Yadav, J., Akinpelu, A., Alnaim, A., et al. (2023). Metronomic Administration of Topotecan Alone and in combination with Docetaxel inhibits epithelial-mesenchymal transition in aggressive variant prostate cancers. *Cancer Res Commun*, 3(7), 1286–1311. <https://doi.org/10.1158/2767-9764.CRC-22-0427>.
157. Bao, M., Xie, J., Piruska, A., & Huck, W. T. S. (2017). 3D microniches reveal the importance of cell size and shape. *Nature Communications*, 8(1), 1962. <https://doi.org/10.1038/s41467-017-02163-2>.
158. Bao, M., Xie, J., Katoe, N., Hu, X., Wang, B., Piruska, A., et al. (2019). Cellular volume and Matrix Stiffness Direct Stem Cell Behavior in a 3D Microniche. *Acs Applied Materials & Interfaces*, 11(2), 1754–1759. <https://doi.org/10.1021/acsami.8b19396>.
159. Lee, H. P., Alisafaei, F., Adebawale, K., Chang, J., Shenoy, V. B., & Chaudhuri, O. (2021). The nuclear piston activates mechanosensitive ion channels to generate cell migration paths in confining microenvironments. *Science Advances*, 7(2). <https://doi.org/10.1126/sciadv.abd4058>.
160. Hemmati, F., Akinpelu, A., Song, J., Amiri, F., McDaniel, A., McMurray, C., et al. (2023). Downregulation of YAP Activity restricts P53 hyperactivation to Promote Cell Survival in Confinement. *Adv Sci (Weinh)*, e2302228. <https://doi.org/10.1002/advs.202302228>.
161. Bera, K., Kiepas, A., Godet, I., Li, Y., Mehta, P., Ifemembu, B., et al. (2022). Extracellular fluid viscosity enhances cell migration and cancer dissemination. *Nature*, 611(7935), 365–373. <https://doi.org/10.1038/s41586-022-05394-6>.
162. Stroka, K. M., Jiang, H., Chen, S. H., Tong, Z., Wirtz, D., Sun, S. X., et al. (2014). Water permeation drives tumor cell migration in confined microenvironments. *Cell*, 157(3), 611–623. <https://doi.org/10.1016/j.cell.2014.02.052>.
163. Zhang, Y., Li, Y., Thompson, K. N., Stoletov, K., Yuan, Q., Bera, K., et al. (2022). Polarized NHE1 and SWELL1 regulate migration direction, efficiency and metastasis. *Nature Communications*, 13(1), 6128. <https://doi.org/10.1038/s41467-022-33683-1>.
164. Pages, D. L., Dornier, E., de Seze, J., Gontran, E., Maitra, A., Maciejewski, A., et al. (2022). Cell clusters adopt a collective amoeboid mode of migration in confined nonadhesive environments. *Science Advances*, 8(39), eabp8416. <https://doi.org/10.1126/sciadv.abp8416>.
165. Holle, A. W., Kutty Devi, G., Clar, N., Fan, K., Saif, A., Kemkemer, T., R., et al. (2019). Cancer cells invade confined microchannels via a Self-Directed Mesenchymal-to-amoeboid transition. *Nano Letters*, 19(4), 2280–2290. <https://doi.org/10.1021/acs.nanolett.8b04720>.
166. Sanz-Moreno, V., Gadea, G., Ahn, J., Paterson, H., Marra, P., Pinner, S., et al. (2008). Rac activation and inactivation control plasticity of tumor cell movement. *Cell*, 135(3), 510–523. <https://doi.org/10.1016/j.cell.2008.09.043>.
167. Pankova, K., Rosel, D., Novotny, M., & Brabek, J. (2010). The molecular mechanisms of transition between mesenchymal and amoeboid invasiveness in tumor cells. *Cellular and Molecular Life Sciences*, 67(1), 63–71. <https://doi.org/10.1007/s0018-009-0132-1>.
168. Graziani, V., Rodriguez-Hernandez, I., Maiques, O., & Sanz-Moreno, V. (2022). The amoeboid state as part of the epithelial-to-mesenchymal transition programme. *Trends in Cell Biology*, 32(3), 228–242. <https://doi.org/10.1016/j.tcb.2021.10.004>.
169. Gao, Y., Wang, Z., Hao, Q., Li, W., Xu, Y., Zhang, J., et al. (2017). Loss of ERalpha induces amoeboid-like migration of breast cancer cells by downregulating vinculin. *Nature Communications*, 8, 14483. <https://doi.org/10.1038/ncomms14483>.
170. Wolf, K., Te Lindert, M., Krause, M., Alexander, S., Te Riet, J., Willis, A. L., et al. (2013). Physical limits of cell migration: Control by ECM space and nuclear deformation and tuning by proteolysis and traction force. *Journal of Cell Biology*, 201(7), 1069–1084. <https://doi.org/10.1083/jcb.201210152>.
171. Harada, T., Swift, J., Irianto, J., Shin, J. W., Spinler, K. R., Athirasala, A., et al. (2014). Nuclear lamin stiffness is a barrier to 3D migration, but softness can limit survival. *Journal of Cell Biology*, 204(5), 669–682. <https://doi.org/10.1083/jcb.201308029>.
172. Davidson, P. M., Sliz, J., Isermann, P., Denais, C., & Lammerding, J. (2015). Design of a microfluidic device to quantify dynamic intra-nuclear deformation during cell migration through confining environments. *Integr Biol (Camb)*, 7(12), 1534–1546. <https://doi.org/10.1039/c5ib00200a>.
173. Lavenus, S. B., Vosatka, K. W., Caruso, A. P., Ullo, M. F., Khan, A., & Logue, J. S. (2022). Emerin regulation of nuclear stiffness is required for fast amoeboid migration in confined environments. *Journal of Cell Science*, 135(8). <https://doi.org/10.1242/jcs.259493>.
174. Bell, E. S., Shah, P., Zuela-Sopilniak, N., Kim, D., Varlet, A. A., Morival, J. L. P., et al. (2022). Low lamin a levels enhance confined cell migration and metastatic capacity in breast

- cancer. *Oncogene*, 41(36), 4211–4230. <https://doi.org/10.1038/s41388-022-02420-9>.
175. McGregor, A. L., Hsia, C. R., & Lammerding, J. (2016). Squish and squeeze—the nucleus as a physical barrier during migration in confined environments. *Current Opinion in Cell Biology*, 40, 32–40. <https://doi.org/10.1016/j.ceb.2016.01.011>.
176. Mistriotis, P., Wisniewski, E. O., Bera, K., Keys, J., Li, Y., Tunithavornwat, S., et al. (2019). Confinement hinders motility by inducing RhoA-mediated nuclear influx, volume expansion, and blebbing. *Journal of Cell Biology*, 218(12), 4093–4111. <https://doi.org/10.1083/jcb.201902057>.
177. Rowat, A. C., Jaalouk, D. E., Zwerger, M., Ung, W. L., Eydelnant, I. A., Olins, D. E., et al. (2013). Nuclear envelope composition determines the ability of neutrophil-type cells to pass through micron-scale constrictions. *Journal of Biological Chemistry*, 288(12), 8610–8618. <https://doi.org/10.1074/jbc.M112.441535>.
178. Kirby, T. J., & Lammerding, J. (2018). Emerging views of the nucleus as a cellular mechanosensor. *Nature Cell Biology*, 20(4), 373–381. <https://doi.org/10.1038/s41556-018-0038-y>.
179. de Leeuw, R., Gruenbaum, Y., & Medalia, O. (2018). Nuclear lamins: Thin filaments with major functions. *Trends in Cell Biology*, 28(1), 34–45. <https://doi.org/10.1016/j.tcb.2017.08.004>.
180. Wintner, O., Hirsch-Attas, N., Schlossberg, M., Brofman, F., Friedman, R., Kupervasser, M., et al. (2020). A unified Linear Viscoelastic Model of the cell nucleus defines the mechanical contributions of Lamins and Chromatin. *Adv Sci (Weinh)*, 7(8), 1901222. <https://doi.org/10.1002/advs.201901222>.
181. Vahabikashi, A., Sivagurunathan, S., Nicdao, F. A. S., Han, Y. L., Park, C. Y., Kittisopkul, M., et al. (2022). Nuclear lamin isoforms differentially contribute to LINC complex-dependent nucleocytoskeletal coupling and whole-cell mechanics. *Proc Natl Acad Sci U S A*, 119(17), e2121816119. <https://doi.org/10.1073/pnas.2121816119>.
182. Stephens, A. D., Liu, P. Z., Banigan, E. J., Almassalha, L. M., Backman, V., Adam, S. A., et al. (2018). Chromatin histone modifications and rigidity affect nuclear morphology independent of lamins. *Molecular Biology of the Cell*, 29(2), 220–233. <https://doi.org/10.1091/mbc.E17-06-0410>.
183. Guilluy, C., Osborne, L. D., Van Landeghem, L., Sharek, L., Superfine, R., Garcia-Mata, R., et al. (2014). Isolated nuclei adapt to force and reveal a mechanotransduction pathway in the nucleus. *Nature Cell Biology*, 16(4), 376–381. <https://doi.org/10.1038/ncb2927>.
184. Bell, E. S., & Lammerding, J. (2016). Causes and consequences of nuclear envelope alterations in tumour progression. *European Journal of Cell Biology*, 95(11), 449–464. <https://doi.org/10.1016/j.ejcb.2016.06.007>.
185. Moir, R. D., Montag-Lowy, M., & Goldman, R. D. (1994). Dynamic properties of nuclear lamins: Lamin B is associated with sites of DNA replication. *Journal of Cell Biology*, 125(6), 1201–1212. <https://doi.org/10.1083/jcb.125.6.1201>.
186. Moir, R. D., Spann, T. P., Herrmann, H., & Goldman, R. D. (2000). Disruption of nuclear lamin organization blocks the elongation phase of DNA replication. *Journal of Cell Biology*, 149(6), 1179–1192. <https://doi.org/10.1083/jcb.149.6.1179>.
187. Vashisth, M., Cho, S., Irianto, J., Xia, Y., Wang, M., Hayes, B., et al. (2021). Scaling concepts in ‘omics: Nuclear lamin-B scales with tumor growth and often predicts poor prognosis, unlike fibrosis. *Proc Natl Acad Sci U S A*, 118(48). <https://doi.org/10.1073/pnas.2112940118>.
188. Raab, M., Gentili, M., de Belly, H., Thiam, H. R., Vargas, P., Jimenez, A. J., et al. (2016). ESCRT III repairs nuclear envelope ruptures during cell migration to limit DNA damage and cell death. *Science*, 352(6283), 359–362. <https://doi.org/10.1126/science.aad7611>.
189. Denais, C. M., Gilbert, R. M., Isermann, P., McGregor, A. L., te Lindert, M., Weigelin, B., et al. (2016). Nuclear envelope rupture and repair during cancer cell migration. *Science*, 352(6283), 353–358. <https://doi.org/10.1126/science.aad7297>.
190. Irianto, J., Xia, Y., Pfeifer, C. R., Athirasala, A., Ji, J., Alvey, C., et al. (2017). DNA damage follows repair factor depletion and portends genome variation in Cancer cells after Pore Migration. *Current Biology*, 27(2), 210–223. <https://doi.org/10.1016/j.cub.2016.11.049>.
191. Takaki, T., Montagner, M., Serres, M. P., Le Berre, M., Russell, M., Collinson, L., et al. (2017). Actomyosin drives cancer cell nuclear dysmorphia and threatens genome stability. *Nature Communications*, 8, 16013. <https://doi.org/10.1038/ncomms16013>.
192. Hatch, E. M., & Hetzer, M. W. (2016). Nuclear envelope rupture is induced by actin-based nucleus confinement. *Journal of Cell Biology*, 215(1), 27–36. <https://doi.org/10.1083/jcb.201603053>.
193. Xia, Y., Pfeifer, C. R., Zhu, K., Irianto, J., Liu, D., Pannell, K., et al. (2019). Rescue of DNA damage after constricted migration reveals a mechano-regulated threshold for cell cycle. *Journal of Cell Biology*, 218(8), 2545–2563. <https://doi.org/10.1083/jcb.201811100>.
194. Xia, Y., Ivanovska, I. L., Zhu, K., Smith, L., Irianto, J., Pfeifer, C. R., et al. (2018). Nuclear rupture at sites of high curvature compromises retention of DNA repair factors. *Journal of Cell Biology*, 217(11), 3796–3808. <https://doi.org/10.1083/jcb.201711161>.
195. Nader, G. P. F., Aguera-Gonzalez, S., Routet, F., Gratia, M., Maurin, M., Cancila, V., et al. (2021). Compromised nuclear envelope integrity drives TREX1-dependent DNA damage and tumor cell invasion. *Cell*, 184(20), 5230–5246e5222. <https://doi.org/10.1016/j.cell.2021.08.035>.
196. Shah, P., Hobson, C. M., Cheng, S., Colville, M. J., Paszek, M. J., Superfine, R., et al. (2021). Nuclear deformation causes DNA damage by increasing replication stress. *Current Biology*, 31(4), 753–765e756. <https://doi.org/10.1016/j.cub.2020.11.037>.
197. Shahbandi, A., Nguyen, H. D., & Jackson, J. G. (2020). TP53 mutations and outcomes in breast Cancer: Reading beyond the headlines. *Trends Cancer*, 6(2), 98–110. <https://doi.org/10.1016/j.trecan.2020.01.007>.
198. Shen, Q., Hill, T., Cai, X., Bui, L., Barakat, R., Hills, E., et al. (2021). Physical confinement during cancer cell migration triggers therapeutic resistance and cancer stem cell-like behavior. *Cancer Letters*, 506, 142–151. <https://doi.org/10.1016/j.canlet.2021.01.020>.
199. Fanfone, D., Wu, Z., Mammi, J., Berthenet, K., Neves, D., Weber, K., et al. (2022). Confined migration promotes cancer metastasis through resistance to anoikis and increased invasiveness. *eLife*, 11, <https://doi.org/10.7554/eLife.73150>.
200. Prentice-Mott, H. V., Chang, C. H., Mahadevan, L., Mitchison, T. J., Irimia, D., & Shah, J. V. (2013). Biased migration of confined neutrophil-like cells in asymmetric hydraulic environments. *Proc Natl Acad Sci U S A*, 110(52), 21006–21011. <https://doi.org/10.1073/pnas.1317441110>.
201. Zanotelli, M. R., Rahman-Zaman, A., VanderBurgh, J. A., Taufalele, P. V., Jain, A., Erickson, D., et al. (2019). Energetic costs regulated by cell mechanics and confinement are predictive of migration path during decision-making. *Nature Communications*, 10(1), 4185. <https://doi.org/10.1038/s41467-019-12155-z>.
202. Zhao, R., Cui, S., Ge, Z., Zhang, Y., Bera, K., Zhu, L., et al. (2021). Hydraulic resistance induces cell phenotypic transition in confinement. *Science Advances*, 7(17). <https://doi.org/10.1126/sciadv.abg4934>.
203. Li, Y., & Sun, S. X. (2018). Transition from actin-driven to Water-Driven Cell Migration depends on External Hydraulic Resistance. *Biophys J*, 114(12), 2965–2973. <https://doi.org/10.1016/j.bpj.2018.04.045>.

204. Yin, J., Kong, X., & Lin, W. (2021). Noninvasive Cancer diagnosis in vivo based on a viscosity-activated Near-Infrared fluorescent probe. *Analytical Chemistry*, 93(4), 2072–2081. <https://doi.org/10.1021/acs.analchem.0c03803>.
205. Ellis, R. J. (2001). Macromolecular crowding: Obvious but underappreciated. *Trends in Biochemical Sciences*, 26(10), 597–604. [https://doi.org/10.1016/s0968-0004\(01\)01938-7](https://doi.org/10.1016/s0968-0004(01)01938-7).
206. Kufe, D. W. (2009). Mucins in cancer: Function, prognosis and therapy. *Nature Reviews Cancer*, 9(12), 874–885. <https://doi.org/10.1038/nrc2761>.
207. von Tempelhoff, G. F., Schonmann, N., Heilmann, L., Pollow, K., & Hommel, G. (2002). Prognostic role of plasmaviscosity in breast cancer. *Clinical Hemorheology and Microcirculation*, 26(1), 55–61.
208. Pittman, M., Iu, E., Li, K., Wang, M., Chen, J., Taneja, N., et al. (2022). Membrane ruffling is a mechanosensor of Extracellular Fluid Viscosity. *Nature Physics*, 18(9), 1112–1121. <https://doi.org/10.1038/s41567-022-01676-y>.
209. Maity, D., Bera, K., Li, Y., Ge, Z., Ni, Q., Konstantopoulos, K., et al. (2022). Extracellular hydraulic resistance enhances Cell Migration. *Adv Sci (Weinh)*, 9(29), e2200927. <https://doi.org/10.1002/advs.202200927>.
210. Lumsden, J. M., Caron, J. P., Steffe, J. F., Briggs, J. L., & Arnoczyk, S. P. (1996). Apparent viscosity of the synovial fluid from mid-carpal, tibiotalar, and distal interphalangeal joints of horses. *American Journal of Veterinary Research*, 57(6), 879–883.
211. Bloomfield, I. G., Johnston, I. H., & Bilston, L. E. (1998). Effects of proteins, blood cells and glucose on the viscosity of cerebrospinal fluid. *Pediatr Neurosurg*, 28(5), 246–251. <https://doi.org/10.1159/000028659>.
212. Marquesich, D. C., Anand, B. S., Lew, G. M., & Graham, D. Y. (1995). Helicobacter pylori infection does not reduce the viscosity of human gastric mucus gel. *Gut*, 36(3), 327–329. <https://doi.org/10.1136/gut.36.3.327>.
213. Rosenson, R. S., McCormick, A., & Uretz, E. F. (1996). Distribution of blood viscosity values and biochemical correlates in healthy adults. *Clinical Chemistry*, 42(8 Pt 1), 1189–1195.
214. Munson, J. M., & Shieh, A. C. (2014). Interstitial fluid flow in cancer: Implications for disease progression and treatment. *Cancer Manag Res*, 6, 317–328. <https://doi.org/10.2147/CMAR.S65444>.
215. Butler, T. P., Grantham, F. H., & Gullino, P. M. (1975). Bulk transfer of fluid in the interstitial compartment of mammary tumors. *Cancer Research*, 35(11 Pt 1), 3084–3088.
216. Klarhofer, M., Csapo, B., Balassy, C., Szentes, J. C., & Moser, E. (2001). High-resolution blood flow velocity measurements in the human finger. *Magnetic Resonance in Medicine*, 45(4), 716–719. <https://doi.org/10.1002/mrm.1096>.
217. Gabe, I. T., Gault, J. H., Ross, J. Jr., Mason, D. T., Mills, C. J., Schillingford, J. P., et al. (1969). Measurement of instantaneous blood flow velocity and pressure in conscious man with a catheter-tip velocity probe. *Circulation*, 40(5), 603–614. <https://doi.org/10.1161/01.cir.40.5.603>.
218. Ivanov, K. P., Kalininina, M. K., & Levkovich Yu, I. (1981). Blood flow velocity in capillaries of brain and muscles and its physiological significance. *Microvascular Research*, 22(2), 143–155. [https://doi.org/10.1016/0026-2862\(81\)90084-4](https://doi.org/10.1016/0026-2862(81)90084-4).
219. Turitto, V. T. (1982). Blood viscosity, mass transport, and thrombogenesis. *Prog Hemost Thromb*, 6, 139–177.
220. Yankaskas, C. L., Bera, K., Stoletov, K., Serra, S. A., Carrillo-Garcia, J., Tuntithavornwat, S., et al. (2021). The fluid shear stress sensor TRPM7 regulates tumor cell intravasation. *Science Advances*, 7(28). <https://doi.org/10.1126/sciadv.abh3457>.
221. Regmi, S., Fu, A., & Luo, K. Q. (2017). High Shear stresses under Exercise Condition destroy circulating Tumor cells in a Microfluidic System. *Scientific Reports*, 7, 39975. <https://doi.org/10.1038/srep39975>.
222. Mitchell, M. J., & King, M. R. (2013). Fluid shear stress sensitizes Cancer cells to receptor-mediated apoptosis via Trimeric Death receptors. *New Journal of Physics*, 15, 015008. <https://doi.org/10.1088/1367-2630/15/1/015008>.
223. Mitchell, M. J., Denais, C., Chan, M. F., Wang, Z., Lammerding, J., & King, M. R. (2015). Lamin A/C deficiency reduces circulating tumor cell resistance to fluid shear stress. *American Journal of Physiology. Cell Physiology*, 309(11), C736–746. <https://doi.org/10.1152/ajpcell.00050.2015>.
224. Xin, Y., Li, K., Yang, M., & Tan, Y. (2020). Fluid shear stress induces EMT of circulating Tumor cells via JNK Signaling in Favor of their survival during Hematogenous Dissemination. *International Journal of Molecular Sciences*, 21(21). <https://doi.org/10.3390/ijms21218115>.
225. Choi, H. Y., Yang, G. M., Dayem, A. A., Saha, S. K., Kim, K., Yoo, Y., et al. (2019). Hydrodynamic shear stress promotes epithelial-mesenchymal transition by downregulating ERK and GSK3beta activities. *Breast Cancer Research*, 21(1), 6. <https://doi.org/10.1186/s13058-018-1071-2>.
226. Riehl, B. D., Kim, E., Lee, J. S., Duan, B., Yang, R., Donahue, H. J., et al. (2020). The role of Fluid Shear and metastatic potential in breast Cancer Cell Migration. *Journal of Biomechanical Engineering*, 142(10). <https://doi.org/10.1115/1.4047076>.
227. Xiong, N., Li, S., Tang, K., Bai, H., Peng, Y., Yang, H., et al. (2017). Involvement of caveolin-1 in low shear stress-induced breast cancer cell motility and adhesion: Roles of FAK/Src and ROCK/p-MLC pathways. *Biochim Biophys Acta Mol Cell Res*, 1864(1), 12–22. <https://doi.org/10.1016/j.bbamcr.2016.10.013>.
228. Zhang, B., Li, X., Tang, K., Xin, Y., Hu, G., Zheng, Y., et al. (2023). Adhesion to the Brain Endothelium selects breast Cancer cells with brain metastasis potential. *International Journal of Molecular Sciences*, 24(8). <https://doi.org/10.3390/ijms24087087>.
229. Follain, G., Osmani, N., Azevedo, A. S., Allio, G., Mercier, L., Karreman, M. A., et al. (2018). Hemodynamic forces Tune the arrest, adhesion, and extravasation of circulating Tumor cells. *Developmental Cell*, 45(1), 33–52. <https://doi.org/10.1016/j.devcel.2018.02.015>.
230. Pedersen, J. A., Lichter, S., & Swartz, M. A. (2010). Cells in 3D matrices under interstitial flow: Effects of extracellular matrix alignment on cell shear stress and drag forces. *Journal of Biomechanics*, 43(5), 900–905. <https://doi.org/10.1016/j.jbiomech.2009.11.007>.
231. Polacheck, W. J., Charest, J. L., & Kamm, R. D. (2011). Interstitial flow influences direction of tumor cell migration through competing mechanisms. *Proc Natl Acad Sci U S A*, 108(27), 11115–11120. <https://doi.org/10.1073/pnas.1103581108>.
232. Haessler, U., Teo, J. C., Foretay, D., Renaud, P., & Swartz, M. A. (2012). Migration dynamics of breast cancer cells in a tunable 3D interstitial flow chamber. *Integr Biol (Camb)*, 4(4), 401–409. <https://doi.org/10.1039/clib00128k>.
233. Shields, J. D., Fleury, M. E., Yong, C., Tomei, A. A., Randolph, G. J., & Swartz, M. A. (2007). Autologous chemotaxis as a mechanism of tumor cell homing to lymphatics via interstitial flow and autocrine CCR7 signaling. *Cancer Cell*, 11(6), 526–538. <https://doi.org/10.1016/j.ccr.2007.04.020>.
234. Polacheck, W. J., German, A. E., Mammoto, A., Ingber, D. E., & Kamm, R. D. (2014). Mechanotransduction of fluid stresses governs 3D cell migration. *Proc Natl Acad Sci U S A*, 111(7), 2447–2452. <https://doi.org/10.1073/pnas.1316848111>.
235. Tien, J., Truslow, J. G., & Nelson, C. M. (2012). Modulation of invasive phenotype by interstitial pressure-driven convection in aggregates of human breast cancer cells. *PLoS One*, 7(9), e45191. <https://doi.org/10.1371/journal.pone.0045191>.

236. Tien, J., Dance, Y. W., Ghani, U., Seibel, A. J., & Nelson, C. M. (2021). Interstitial hypertension suppresses escape of human breast tumor cells via Convection of interstitial fluid. *Cellular and Molecular Bioengineering*, 14(2), 147–159. <https://doi.org/10.1007/s12195-020-00661-w>.
237. Piotrowski-Daspit, A. S., Tien, J., & Nelson, C. M. (2016). Interstitial fluid pressure regulates collective invasion in engineered human breast tumors via snail, vimentin, and E-cadherin. *Integr Biol (Camb)*, 8(3), 319–331. <https://doi.org/10.1039/c5ib00282f>.
238. Huang, Y. L., Tung, C. K., Zheng, A., Kim, B. J., & Wu, M. (2015). Interstitial flows promote amoeboid over mesenchymal motility of breast cancer cells revealed by a three dimensional microfluidic model. *Integr Biol (Camb)*, 7(11), 1402–1411. <https://doi.org/10.1039/c5ib00115c>.
239. Yankaskas, C. L., Thompson, K. N., Paul, C. D., Vitolo, M. I., Mistriotis, P., Mahendra, A., et al. (2019). A microfluidic assay for the quantification of the metastatic propensity of breast cancer specimens. *Nat Biomed Eng*, 3(6), 452–465. <https://doi.org/10.1038/s41551-019-0400-9>.
240. Patel, B. K., Samreen, N., Zhou, Y., Chen, J., Brandt, K., Ehman, R., et al. (2021). MR Elastography of the breast: Evolution of technique, case examples, and future directions. *Clinical Breast Cancer*, 21(1), e102–e111. <https://doi.org/10.1016/j.clbc.2020.08.005>.

**Publisher's Note** Springer Nature remains neutral with regard to jurisdictional claims in published maps and institutional affiliations.